Title

Delta opioid receptor activation modulates affective pain and modality-specific pain hypersensitivity associated with chronic neuropathic pain

Journal

Journal of Neuroscience Research, 100(1)

ISSN

0360-4012

Authors

Cahill, Catherine M
Holdridge, Sarah V
Liu, Shiwei
et al.

Publication Date

2022

DOI

10.1002/jnr.24680

Peer reviewed

Received: 25 February 2020 | Revised: 28 April 2020 | Accepted: 4 June 2020

DOI: 10.1002/jnr.24680

RESEARCH ARTICLE

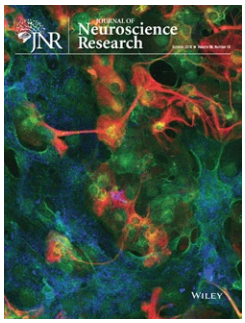

Delta opioid receptor activation modulates affective pain and modality-specific pain hypersensitivity associated with chronic neuropathic pain

Catherine M. Cahill[1] | Sarah V. Holdridge[2] | Shiwei (Steve) Liu[1] | Lihua Xue[2] | Claire Magnussen[2] | Edmund Ong[2] | Patrick Grenier[2] | Anne Sutherland[2] | Mary C. Olmstead[3]

[1]Department of Psychiatry & Biobehavioral Sciences, Hatos Center for Neuropharmacology, Semel Institute for Neuroscience and Human Behavior, University of California Los Angeles, Los Angeles, CA, USA

[2]Department of Pharmacology & Toxicology, Queen's University, Kingston, ON, Canada

[3]Department of Psychology and Centre for Neuroscience Studies, Queen's University, Kingston, ON, Canada

Correspondence
Catherine M. Cahill, Department of Psychiatry and Biobehavioral Sciences, Semel Institute for Neuroscience and Human Behavior, Shirley and Stefan Hatos Center for Neuropharmacology, MacDonald Research Laboratory Building, 675 Charles E Young Drive South, Office 2774, Mail Code: 175919, Los Angeles, CA 90095, USA.
Email: cmcahill@ucla.edu

Funding information
Canadian Foundation for Innovation; NIH-National Institute of Drug Abuse, Grant/Award Number: 1UG3TR003148-01, 2P50 DA005010 and R01DA041781; Canadian Network for Research and Innovation in Machining Technology, Natural Sciences and Engineering Research Council of Canada; Ontario Innovation Trust; Department of Defense, United States Government, Grant/Award Number: W81XWH-15-1-0435; J.P. Bickell Foundation; Canada Research Chairs; University of California, Irvine; Ontario Graduate Scholarship in Science & Technology; Shirley and Stefan Hatos Foundation; Institute of Neurosciences, Mental Health and Addiction, Grant/Award Number: MOP 123298

Abstract

Delta opioid receptor (DOR) agonists alleviate nociceptive behaviors in various chronic pain models, including neuropathic pain, while having minimal effect on sensory thresholds in the absence of injury. The mechanisms underlying nerve injury-induced enhancement of DOR function are unclear. We used a peripheral nerve injury (PNI) model of neuropathic pain to assess changes in the function and localization of DORs in mice and rats. Intrathecal administration of DOR agonists reversed mechanical allodynia and thermal hyperalgesia. The dose-dependent thermal antinociceptive effects of DOR agonists were shifted to the left in PNI rats. Administration of DOR agonists produced a conditioned place preference in PNI, but not in sham, animals, whereas the DOR antagonist naltrindole produced a place aversion in PNI, but not in sham, mice, suggesting the engagement of endogenous DOR activity in suppressing pain associated with the injury. GTPγS autoradiography revealed an increase in DOR function in the dorsal spinal cord, ipsilateral to PNI. Immunogold electron microscopy and *in vivo* fluorescent agonist assays were used to assess changes in the ultrastructural localization of DORs in the spinal dorsal horn. In shams, DORs were primarily localized within intracellular compartments. PNI significantly increased the cell surface expression of DORs within lamina IV-V dendritic profiles. Using neonatal capsaicin treatment, we identified that DOR agonist-induced thermal antinociception was mediated via receptors expressed on primary afferent sensory neurons but did not alter mechanical thresholds. These data reveal that the regulation of DORs

Edited by Tuan Trang. Reviewed by John Streicher, Emily Jutkiewicz, Erin Bobeck, and Mariana Lemos Duarte.

The peer review history for this article is available at https://publons.com/publon/10.1002/jnr.24680.

following PNI and suggest the importance of endogenous activation of DORs in regulating chronic pain states.

KEYWORDS

capsaicin, chronic pain, dorsal root ganglia, neuropathic pain, nociception, opiate, opioid, opioid receptor, pain, pain unpleasantness, peripheral nerve injury, spinal cord

1 | INTRODUCTION

Nearly 50% of Americans visit a physician with a principal complaint of pain each year (Katz, 2002), but chronic pain is recognized as an independent disease process, necessitating both symptom relief and mechanism-based therapy. Poorly controlled pain can be extremely debilitating and can have a profoundly negative impact on overall quality of life. Neuropathic pain, resulting from injury or damage to a peripheral or central nerve, is particularly undermanaged in the clinical setting. It is characterized by hyperalgesia (an exaggerated response to a noxious stimulus), allodynia (perceived pain to an innocuous stimulus), and spontaneous pain (pain in the absence of a known stimulus). First-line therapies include traditional mu opioid receptor (MOR) agonist drugs, as well as nontraditional analgesics, such as tricyclic antidepressants and anticonvulsants (Gilron, Watson, Cahill, & Moulin, 2006). However, the potential abuse liability or ineffectiveness of current pain medications has prompted a sustained and collaborative research effort with the goal of developing novel treatment strategies and understanding the molecular mechanisms and changes in circuitry in the genesis and persistence of chronic pain states.

Significance

Using behavioral assays, ultrastructural analysis, ligand internalization, and autoradiography, we demonstrate that neuropathic pain increases the expression pattern and function of delta opioid receptors (DORs) that play an important role in modulating nociceptive transmission. Our study shows that activation of DORs modulates both the sensory and affective, unpleasant dimensions of the pain experience, whereby a delta agonist produces a place preference (negative reinforcement) and a delta antagonists produces a place aversion. Using a neurochemical assay and transient receptor potential vanilloid receptor 1 ablation techniques, we show that the DOR expression on primary sensory neurons appears to be important for modulating thermal, but not mechanical nociception.

Studies from our own laboratory and others have identified changes in function and expression of the delta opioid receptor (DOR) in models of chronic pain. While DOR-selective agonists have been shown to produce modest or no antinociception in acute pain tests, they reduce nociception in models of persistent inflammatory and neuropathic pain (Gendron, Cahill, Zastrow, Schiller, & Pineyro, 2016). Indeed, deltorphin II (DLT), a selective DOR agonist, alleviated nociceptive (Holdridge & Cahill, 2007) and mechanical allodynia following local (Kabli & Cahill, 2007) and spinal (Holdridge & Cahill, 2007) administration. Furthermore, behavioral and electrophysiological studies report an increase in DOR functional competence in nerve-injured animals compared with controls (Gendron et al., 2016). DORs are also thought to be responsible for modulating the effectiveness of tricyclic antidepressant drugs in treating neuropathic pain. For example, the anti-allodynic effects of nortriptyline are blocked by the DOR antagonist naltrindole (Benbouzid et al., 2008; Choucair-Jaafar, Salvat, Freund-Mercier, & Barrot, 2014).

Despite the failures of advancing DOR agonists as novel analgesics and their limited success as antidepressant agents (Gendron et al., 2016; Pradhan, Befort, Nozaki, Gavériaux-Ruff, & Kieffer, 2011; Spahn & Stein, 2017; Vicente-Sanchez, Segura, & Pradhan, 2016), there is still much enthusiasm for further development of DOR-selective drugs. For example, Cubist Pharmaceuticals, LLC did not show clinical efficacy in patient with postherpetic neuralgia, osteoarthritis, and rheumatoid arthritis pain. AstraZeneca published results suggested that AZD2327 has larger potential anxiolytic effects than antidepressant drugs, and they concluded that additional research with DOR agonists should be considered (Richards et al., 2016). This exemplifies the need to further understand where and how the DOR can functionally modify nociceptive transmission and the emotional, unpleasant component of pain processing. Further, while most studies agree that chronic pain enhances DOR function, there have been conflicting reports of the mechanism that accounts for the augmented effects of DOR agonists in relevant models. Specifically the extent an increased function occurs either presynaptically on primary afferent terminals or postsynaptically on second-order dorsal horn neurons that are part of the ascending spinothalamic and other nociceptive circuits (Overland et al., 2009; Scherrer et al., 2009).

In the current study, we aimed to investigate whether the peripheral nerve injury (PNI) model of neuropathic pain produces changes in cell surface expression of DORs in the dorsal horn of the rat spinal cord and the extent to which modulation of pain hypersensitivity is due to the localization of receptors in capsaicin-sensitive afferents. Using both neurochemical release and capsaicin allowed us to determine the extent chronic pain modified the function of presynaptic DORs. To investigate cell surface expression, the subcellular distribution of DORs was assessed in laminae I-II and V of dendrites by immunogold electron microscopy. We also assessed the unpleasant

component of chronic pain through the conditioned place preference (CPP) paradigm and the ability of DOR agonists and antagonists to modulate this dimension of chronic pain.

2 | METHODS AND MATERIALS

2.1 | Experimental subjects

All experiments were performed on adult male Sprague Dawley rats (225–250 g at the time of arrival in the vivarium; Charles River, PQ, CAN) or 8- to 12-week-old male and female C57BL/6J mice (Jackson Laboratories, ME). Mice were housed in groups of two to four per cage on a 12-hr reverse light/dark cycle, with food and water available *ad libitum*. Long-Evans rats (250–300 g) were housed in pairs on a 12-hr reverse light/dark cycle, with food and water available *ad libitum*. Rodents were allowed to habituate to their housing environments for 1 week before handling. Experiments were conducted in the dark phase between 9:00 and 14:00 hr. To the extent possible, experimenters handling mice were blind to surgery, genotype, sex, and drug treatment. Importantly, all tests were carried out by experimenters who were blind to experimental conditions. Additionally, all experiments were performed in low-light conditions (LUX 5-40) depending on the experiment. Paw threshold testing was at the higher lux light level while CPP experiments were conducted under red-light conditions. Mice were assigned to experimental conditions in a randomized block design so that factors such as time of day were counterbalanced over the experimental conditions. For experiments that had large numbers of groups, we completed them using successive cohorts, ensuring that experiments were carried out for all conditions within each cohort. All replications were balanced with respect to experimental groups. Species and strain have been identified in the appropriate section below; however, for clarity and transparency, Sprague Dawley rats were used for all nociceptive threshold tests, including neonatal capsaicin treatment and subsequent nociceptive testing. They were also used for electron microscopy experiments. Long-Evans rats were used for CPP, GTPgS, CGRP neurochemical release, and *in vivo* fluorescent DLT internalization. We made the decision to change the strain to Long-Evans for certain experiments, as they are generally more amendable to behavioral tasks involved in learning, which is required for CPP tests. For example, when directly comparing these rat strains, Long-Evans rats required fewer sessions than Sprague Dawley rats to learn operant tasks, including a signal detection task and reversal learning (Turner & Burne, 2014). Mice were used in CPP and aversion studies to determine if results were generalizable across another species.

2.2 | Ethical approval

All procedures were preapproved by the University of California, Irvine Institutional Animal Care and Use Committee, the University of California, Los Angeles Chancellor's Animal Research Council, or the Canadian Council on Animal Care and the Queen's University or University of Calgary Animal Care Committees. All procedures were in accordance with the guidelines set forth by the International Association for the Study of Pain Committee for Research and Ethical Issues.

2.3 | Experimental design and procedures

2.3.1 | Induction of chronic neuropathic pain

Peripheral nerve injury was accomplished by chronic constriction injury to the left sciatic nerve as we have previously described (Liu et al., 2019; Taylor et al., 2015). Briefly, rodents were anesthetized by isoflurane inhalation (5 L/min induction; 2 L/min maintenance). A small incision was made on the upper thigh and the underlying muscle was bluntly dissected. A fixed-diameter polyethylene cuff (PE90 for rats and PE20 for mice) 2 mm in length was placed loosely around the common sciatic nerve, proximal to its bifurcation into the tibial and sural nerves. The muscle was sutured with Vicryl sutures for rats, but was not sutured in mice. Dermal incisions were closed with Monocyrl sutures. Control animals received sham operations, in which identical surgical procedures were used, but without manipulation of the nerve. Behavioral testing was conducted prior to and at 7 and/or 14 days post-surgery. A separate group of animals was used for tissue harvesting on day 14 post-surgery.

2.3.2 | Behavior

Mechanical withdrawal thresholds

Separate groups of Sprague Dawley rats were used in each behavioral testing paradigm. All rodents underwent presurgical behavioral testing in their respective paradigms to establish baseline values to which comparisons could be made post-surgery and postdrug administration. Rodents were then divided into two groups; those that underwent PNI by sciatic nerve constriction or those that underwent sham surgery. Intrathecal administration of all drugs (15 µl volume) was accomplished by lumbar puncture between the L4 and L5 vertebrae under brief isoflurane anesthesia in rats. Anti-allodynic and anti-hyperalgesic effects of the selective DOR agonists D-[Ala^2, Glu^4]deltorphin II (DLT), [D-Ser^2,Leu^5, Thr^6]-enkephalin (DSLET), D-[Pen^2], D-[Pen^5]-enkephalin (DPDPE), and 4-[(*R*)-[(2*S*,5*R*)-4-allyl-2,5-dimethylpiperazin-1-yl](3-methoxyphenyl)methyl]-*N*,*N*-diethylbenzamide (SNC80) were assessed. To determine the stress response that may be result from the lumbar puncture procedure, saline vehicle was administered and the effects were assessed 20 min postinjection. Mechanical withdrawal responses to von Frey filament stimulation were assessed in PNI and sham rats as previously described by Chaplan (Chaplan, Bach, Pogrel, Chung, & Yaksh, 1994). Rats were placed under opaque Plexiglas® boxes positioned on a wire grid platform (5 × 5 mm mesh), through which von Frey filaments were applied to the plantar surface of the hind

paw in an up-down fashion. In brief, filaments were applied in either ascending or descending force as necessary in order to most accurately determine the threshold of response. The intensity of stimuli ranged from 0.25 to 15 g. From the resulting response patterns, the 50% response thresholds (g) were calculated.

Thermal withdrawal thresholds

The anti-hyperalgesic effects of DOR agonists were assessed in PNI and sham Sprague Dawley rats on day 14 post-surgery using the Hargreaves apparatus. Thermal withdrawal latencies were measured following injection for n = 5–7 rats per treatment. A cutoff latency of three times the predrug value was imposed to prevent tissue damage. Anti-hyperalgesic drug effects were assessed by transforming raw latency data into percentage of the maximum possible effect (% M.P.E.) values as follows: % M.P.E. = ((postdrug latency − baseline) ÷ (cutoff latency − baseline)) × 100. Thermal nociception was determined using a hot water tail flick apparatus. Rats were gently restrained by cupping them in an infant baby sock, then 2.5 cm of the tail was immersed in a 49°C water bath. The time to tail withdrawal was measured. After three basal measurements were taken at least 5 min apart, mice were injected with morphine (0.1–10 mg/kg, i.p.) or DLT (1–30 μg/intrathecal injection). Tail withdrawal latencies were measured every 10 min for 1 hr. Rats were returned to their home cages between testing. A cutoff of 15 s was imposed to avoid tissue damage based on baseline latencies of 4–6 s. Dose-dependent effects were determined at peak antinociceptive responses for each drug (20 min following DLT or 30 min following morphine administration).

Conditioned place preference/conditioned place aversion

The place preference paradigm was conducted using an unbiased, counterbalanced, three-chamber apparatus. Each square-floored box (28 × 28 × 19 cm) was divided into two equal-sized conditioning chambers connected by a neutral chamber. The two conditioning chambers were distinguishable by visual and tactile cues using two types of metal flooring. In order to counterbalance the groups before the conditioning sessions, mice were placed in the CPP apparatus and allowed free access to both chambers. The time spent in each chamber was recorded over 30 min using an infrared CCD camera attached to a computer running behavioral tracking software (Noldus Ethovision, Leesberg, VA). The drug-paired chamber was assigned such that any innate bias for one chamber over the other was balanced among treatment groups. Conditioning sessions consisted of Long-Evans rats (N = 10–12 per group) or mice (n = 8–12 per group) receiving eight conditioning sessions, with 4 days of drug and 4 days of vehicle (saline) conditioning that consisted of confinement in the appropriate chamber for 30 min. The CPP assay began 7 days after surgery with conditioning beginning on day 9 after pain onset, a time point consistent with maximal pain behavior (Liu et al., 2019; Taylor et al., 2015). For Long-Evans rats, drug conditioning was performed with intrathecal administration of DLT (30 μg/injection) or intrathecal saline on alternate days. For mice, drug conditioning was performed with SNC80 (5 mg/kg, i.p.); a separate cohort received naltrindole (5 mg/kg, i.p.). On the postconditioning day, animals were allowed free access to all chambers in a drug-free state, and the time spent in the drug-paired chamber was measured over 30 min. Data are presented as times spent in each conditioning chamber.

2.3.3 | Agonist-stimulated GTPγS autoradiography

Brains were collected from sham and PNI Long-Evans rats 2 weeks post-surgery. Brains were snap-frozen with isopentane at −30°C, then stored at −80°C until further processing. On the day of processing, brains were sectioned coronally using a cryostat (20 μm thick sections) at −20°C. Sections were thaw-mounted on SuperFrost charged slides. Sections were preincubated in assay buffer (50 mM tris-HCl, 3 mM $MgCl_2$, 0.2 mM EGTA, 100 mM NaCl, 2 mM GDP, 1 μM DPCPX, pH 7.4) for 15 min. Agonist-stimulated DOR activity was determined by incubating brain sections in [^{35}S]GTPγS (40 pM) with the DOR agonist SNC80 (10 μM) alone or in combination with the DOR antagonist SDM25N (10 μM) for 1 hr at room temperature (RT). After incubation, slides were washed two times in ice-cold wash buffer (50 mm tris-HCl, pH 7.4), followed by a brief wash in ice-cold deionized water (30 s). Slides were air-dried, then exposed to Kodak Biomax film along with [^{14}C] standards for 2 days. Films were developed using a Kodak GBX Developer and RapidFix solution. Films were digitally analyzed, and binding was quantified using a MicroComputer Image Device (MCID), normalized to a [^{14}C] standard curve in dpm/mg (MCID Imaging Research, St. Catherine, Ontario, Canada). Data from the resulting agonist-stimulated samples were compared to nonagonist-treated brain samples to determine the percent activation of DOR above basal levels.

2.3.4 | *In vivo* fluorescent deltorphin internalization assay

Internalized fluorescent DOR agonist, ω-Bodipy 576/589 deltorphin-I 5-aminopentylamide (Fluo-DLT) was visualized in the Long-Evans rat lumbar (L4–5) spinal cord using confocal microscopy as previously demonstrated (Gendron et al., 2007; Morinville et al., 2004). Sham or neuropathic rats (day 14 post-surgery) were anesthetized with sodium pentobarbital (70 mg/kg, i.p.) and injected, intrathecally, via a lumbar puncture with 0.8 nmol Fluo-DLT under brief isoflurane anesthesia. Previous studies have demonstrated specificity of this concentration of Fluo-DLT, as internalization was completely blocked by pretreatment with the opioid receptor antagonist naloxone (Morinville et al., 2004). Rats were sacrificed 20 min after injection of the fluorescent-tagged ligand by intra-aortic arch perfusion of 4% paraformaldehyde (PFA) in 0.1 M phosphate buffer (PB; 500 ml, pH 7.4) at 4°C, followed by 10% sucrose in 0.2 M PB (100 ml, pH 7.4), 20% sucrose in 0.2 M PB (100 ml, pH 7.4), and 30% sucrose in 0.2 M PB (100 ml, pH 7.4). Lumbar segments of the spinal cord were snap-frozen in isopentane at −45°C, placed on dry ice, and immediately processed for cryostat sectioning. Frozen tissue

was transversely cut at the L4–5 lumbar segment at a thickness of 20 μm and thaw-mounted onto chrome alum/gelatin-coated slides. Sections were visualized and imaged (without coverslips) using a Leica TCS SP2 multi-photon confocal microscope (63× magnification; Leica Microsystems, Inc.). Representative images were acquired within laminae IV-V for eight to ten sections per animal. Perikaryal profiles displaying internalized Fluo-DLT (i.e., intracytoplasmic fluorescent puncta) within each lamina were counted in three animals per experimental condition, ensuring that section thickness, number of sections sampled (N = 8–10 per animal), and acquisition parameters were constant between paired experimental groups. Global fluorescence intensity levels over entire confocal microscopic images were quantified (by an experimenter blinded to treatments) following conversion of the images to gray scale. Subsequently, using the thresholding function of Image J software (National Institutes of Health (NIH), USA), the fluorescence-labeling levels were expressed in arbitrary units (AU). Calculations and statistical analyses were performed using GraphPad Prism software (version 8.0).

2.3.5 | Calcitonin gene-related peptide (CGRP) release from spinal cord slices

Sham and PNI (14 days post-surgery) Long-Evans rats were decapitated and their spinal cords were rapidly removed by hydrostatic propulsion. The L4/L5 spinal cord was immediately placed in ice-cold, oxygenated (95% O_2, 5% CO_2) Krebs buffer (NaCl 135 mM, KCl 3.5 mM, $MgSO_4$ 1 mM, NaH_2PO_4 1 mM, $NaHCO_3$ 20 mM, $CaCl_2$ 2.5 mM, dextrose 3.3 mM, ascorbic acid 0.2 mM, thiorphan 20 μM, and bovine serum albumin (BSA) 0.1%). Spinal cord segments were hemisected sagittally into ipsilateral and contralateral sections and cut with a tissue chopper into 400-μm thick sections. Dorsal horn spinal lumbar segments were transferred to an incubation chamber and continuously perfused (0.3 ml/min) with warm (37°C), oxygenated Krebs buffer. After allowing 45 min for equilibration, superfusate fractions were collected at 5 min intervals. After collecting four basal fractions (over 20 min), sections were stimulated with capsaicin (300 nM in Krebs buffer), with and without the DOR agonist DLT (10 μM) to evoke release of CGRP. Superfusates were collected every 5 min for 10 min before switching back to Krebs buffer. The superfusates were stored at −80°C until use, then subjected to an SPI-Bio CGRP enzyme immunoassay kit (Cayman Chemical) to determine the CGRP concentrations based on a standard curve.

2.3.6 | Subcellular localization of DOR

Fourteen days after surgery, Sprague Dawley rats were deeply anesthetized with sodium pentobarbital and transaortically perfused at 45 ml/min with 100 ml of heparinized saline (6 U/ml heparin), followed by a solution containing 3.75% acrolein and 2% PFA in 60 ml of 0.1 M PB, pH 7.4, and finally with 400 ml of 2% PFA in 0.1 M PB. Lumbar spinal cords were removed and postfixed in the same 2% PFA solution. Transverse sections (50 μm) were cut using a vibratome and processed for DOR immunogold labeling as described previously (Cahill, McClellan, et al., 2001; Cahill, Morinville, et al., 2001). Sections were incubated with 1% sodium borohydride in PB for 30 min to neutralize free aldehyde groups to improve antigen recognition. Sections were cryoprotected and subjected to a freeze-thaw protocol consisting of isopentane (–70°C) and liquid nitrogen. Following incubation with 3% NGS, sections were then incubated with DOR antisera in TBS containing 0.5% NGS for 36 hr at 4°C. Antibody specificity and analysis can be found in Supporting Information (Figure S1). Control sections were processed in the absence of primary antibody. After rinsing, sections were incubated with colloidal gold (1 nm)-conjugated goat anti-rabbit immunoglobulin G (IgG; AuroProbe One GAR, Amersham Pharmacia Biotech, Baie D'Ufré, QC, CAN) for 2 hr at RT. Sections were fixed with 2% glutaraldehyde prior to amplification of immunogold particle labeling by silver intensification for 10 min (IntenSE M Silver Enhancement Kit, Amersham Pharmacia Biotech). The reaction was terminated by the application of 0.2 M citrate buffer, pH 7.4. Sections were postfixed and stained for 40 min with 2% osmium tetroxide in PB, dehydrated in graded alcohol concentrations, and finally embedded in Epon 812 resin. Ultrathin sections (80 nm) were prepared and collected on copper grids, then counter-stained with uranyl acetate and lead citrate for visualization with a Hitachi transmission electron microscope at 15,000× magnification. Negatives were digitized using an Epson Perfection 4990 photo scanner and images were processed using Photoshop 7.0 (Adobe Systems Inc., San Jose, CA, USA).

Quantification of DOR subcellular distribution was accomplished using ImageJ 1.36b (NIH, USA). A minimum of 40 immunopositive dendritic profiles containing three or more gold particles were imaged within laminae I-II and V from the ipsilateral and contralateral dorsal horn regions for n = 6 experiments per condition. The copper grids were coded and the experimenter was blinded to the sample conditions. The perimeter and cross-sectional area of each dendrite was measured. Within each dendrite, gold particles were counted and classified as being either plasma membrane-associated or intracellular (cytosolic). Particles were considered membrane-associated if they were overlying or in direct contact with the plasma membrane, while all other particles were considered intracellular. For those gold particles deemed intracellular, the linear distance between the particle and the closest point of the plasma membrane was measured. From these data, the following calculations were made: (a) average number of gold particles counted per dendrite, (b) percentage of total gold particles associated with the plasma membrane, (c) percentage of total dendrites with plasma membrane-associated gold particles, (d) average distance of intracellular particles from the plasma membrane. All data represent means ± standard error of the mean (*SEM*). Data were analyzed by one-way ANOVAs followed by *post hoc* analysis using Tukey's multiple comparison tests (MCTs) or unpaired two-tailed *t*-tests, where appropriate. Details of each analysis are provided in the Results section. All data calculations, analyses and graphs were prepared using Microsoft Excel XP and GraphPad Prism 5.0.

2.3.7 | Neonatal capsaicin treatment

In order to assess the role of capsaicin-sensitive nociceptive afferents, Sprague Dawley rat pups were anesthetized on ice and administered capsaicin or vehicle on the first and second postnatal days (25 mg/kg and 50 mg/kg in 50 µl of 60% dimethyl sulfoxide (DMSO), s.c.; Sigma). Pups were housed with the dam until weaning at 21 days, after which they were housed in pairs. At approximately 250 g body weight (8 weeks of age), mature male rats underwent PNI surgery, or not, for behavioral and immunohistochemical analyses.

2.3.8 | Immunohistochemistry for fluorescence microscopy

To assess the loss of nociceptive afferent cell populations in adult Sprague Dawley rats following neonatal capsaicin treatment, fluorescent detection of specific cell markers was carried out using immunohistochemical techniques. Rats were anesthetized with sodium pentobarbital (75 mg/kg, i.p.) and perfusion-fixed through the aortic arch with 500 ml of 4% PFA in 0.1 M PB (pH 7.4). Lumbar spinal cords were isolated and postfixed in 4% PFA in 0.1 M PB for 30 min at 4°C, followed by cryoprotection in 30% sucrose in 0.1 M PB for 48 hr at 4°C. Spinal cords were cut into 40-µm transverse sections on a freezing sledge microtome, and free-floating sections were processed for immunodetection of CGRP (1:1,000, Bachem, Torrance, CA), substance P (SP; 1:1,000, Chemicon, Temecular, CA), and the *Griffonia simplicifolia* isolectin B4 (IB4; 1:200, Sigma). Briefly, sections were rinsed in 0.1 M TBS, then incubated in 3% NGS in 0.1 M TBS for 1 hr at RT. Sections were then incubated with the primary antibodies, diluted in 1% NGS in 0.1 M TBS as follows: anti-SP for 48 hr at 4°C, anti-CGRP for 24 hr at 4°C. Following rinses with 0.1 M TBS, sections were incubated with the appropriate secondary antisera conjugated to either Alexa-594 or −488 fluorophores (all 1:200, Molecular Probes, Invitrogen, ON, CA) for 2 hr at RT in the dark. The lectin antibody used to label IB4 was directly conjugated to fluorescein isothiocyanate (FITC) and was administered in 1% NGS in 0.1 M TBS at the same time as the secondary antisera. Finally, sections were rinsed with 0.1 M TBS, mounted onto glass Superfrost microscope slides and coverslipped with Aquamount (Polysciences, Canada). Spinal cord sections were visualized on a Leica DM 4000 microscope (5× magnification; Leica Microsystems Inc, ON, Canada) and imaged using a Leica DFC 350 FX digital camera (Leica Microsystems) and OpenLab 4.01 software (Improvision/Quorum Technologies, Guelph, CA). Quantification of immunolabeling was carried out by densitometric measurement of mean density values using Image J software (NIH, USA). Four spinal cord sections were randomly selected from N = 7–9 rats in each treatment group. Mean intensity values in the dorsal horn region of all treatment groups are expressed as means ± *SEM*, and were compared by one-way ANOVA followed by Bonferroni's *post hoc* MCT.

2.3.9 | Statistics and data analysis

Data are either expressed as scatter plots for raw data and bar graphs showing means ± *SEM*s or as medians with 25% and 75% quartiles, with minimum and maximum data points. Data were analyzed by GraphPad Prism v7.0 or 8.4. All behavioral data met the assumptions of a general linear model and were subjected to Factorial ANOVAs. All behavioral data were analyzed by one- or two-way ANOVAs followed by Dunnett's *post hoc* test or Bonferroni's or Sidak's MCTs, where appropriate. Dose–response curves were analyzed by nonlinear regression (curve fit) using a dose–response stimulation to generate ED50 values and Confidence intervals. For CPP data, the amount of time (s) spent in the drug-paired and vehicle-paired compartments on the postconditioning test day is presented, and CPP data were analyzed by paired *t*-tests. A two-way ANOVA with drug dose and surgical group as the between-subject factors was used to examine differences in the magnitude of preference or aversion across groups. Details of each analysis are provided in the Results section. A two-way ANOVA with drug dose and surgical group as the between-subject factors was used to examine differences in the magnitude of CPP or conditioned place aversion (CPA) across neuropathic pain, sham, and pain-naive groups, followed by Tukey's *post hoc* analysis for multiple comparisons. p values <0.05 were deemed statistically significant.

3 | RESULTS

3.1 | Anti-allodynic, anti-hyperalgesic, and antinociceptive effects of DOR agonists

To determine the ability of DOR agonists to modulate nociception associated with PNI, four DOR agonists were administered intrathecally on day 14 following surgery. Prior to surgery, all Sprague Dawley rats were unresponsive to mechanical stimuli up to the maximum tactile force of 15.0 g, indicative of the innocuous nature of the stimulus. Following surgery, PNI rats displayed a significant decrease in mechanical withdrawal thresholds in the ipsilateral hind paw, interpreted as the development of mechanical allodynia, with no change in withdrawal thresholds of the contralateral hind paw over time. Mechanical withdrawal thresholds were determined prior to and 20 min following drug administration. All agonists tested, including peptide-based agonists DPDPE (10 µg), DLT (30 µg), and DSLET (10 µg), and the non-peptide agonist SNC80 (30 µg), significantly attenuated mechanical allodynia assessed by von Frey filaments (Figure 1a). Sham animals displayed mechanical thresholds that were already at the upper cutoff of threshold detection (~15 g), preventing assessment of the nociceptive effects of the DOR agonists in this test (Figure S2).

Intrathecal administration of DLT produced significant anti-hyperalgesia in the ipsilateral hind paws of PNI Sprague Dawley rats, compared with saline vehicle, at 20, 30, and 50 min postinjection (two-way ANOVA, Bonferroni MCT, $F_{12, 30} = 16.52$, $^*p < 0.001$), as well as significant analgesia in the contralateral hind paws of PNI rats

at 20 and 50 min postinjection (two-way ANOVA, Bonferroni MCT, $F_{12, 30} = 5.854$, $^{*}p < 0.01$). The antinociceptive effects of DLT in sham rats were not different from saline. The effects of DLT were significantly greater in the ipsilateral hind paws of PNI rats than in sham rats, whereas no significantly difference was observed on the contralateral side (Figure 1b). The effects of saline were negligible in both groups, indicating no effect of lumbar puncture or the injection itself.

The antinociceptive effects of intrathecal morphine or DLT were assessed using the hot water tail flick test on postsurgical day 7 (Figure 1c). Both drugs produced dose-dependent analgesia in both

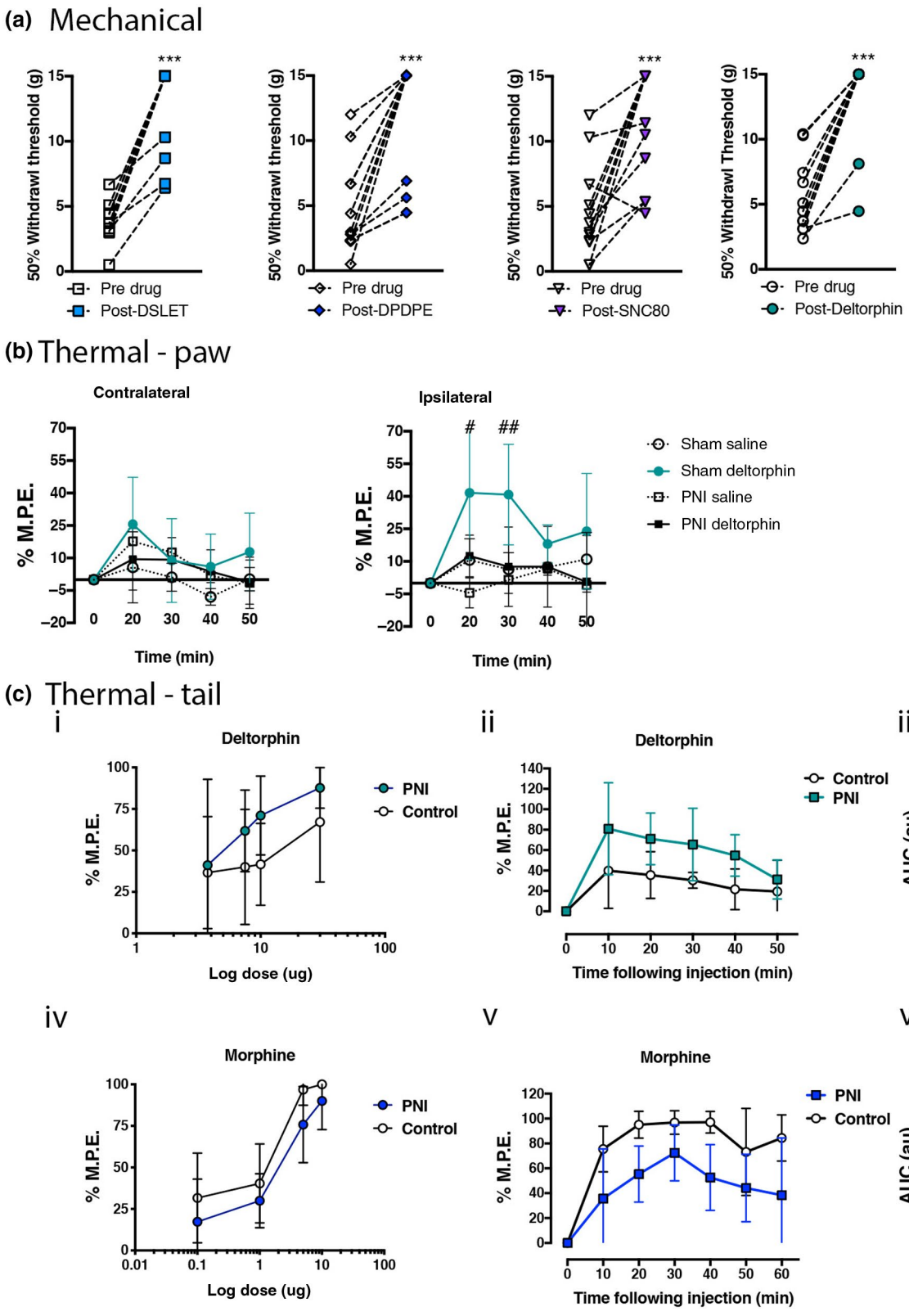

FIGURE 1 DOR agonists attenuate mechanical hypersensitivity and enhance thermal antinociception in neuropathic pain states, whereas morphine antinociception is attenuated by the occurrence of neuropathic pain. (a) Mechanical withdrawal responses were assessed in Sprague Dawley rats with peripheral nerve injury (PNI), prior to and following intrathecal (i.t.) administration of DOR agonists DSLET (10 μg), DPDPE (10 μg), SNC80 (30 μg), and deltorphin (DLT, 10 μg) on day 14 post-surgery. Data represent means ± *SEM* for *N* = 9–12 per group. All DOR agonists attenuated mechanical allodynia in the PNI rat model of neuropathic pain. **p* < 0.05 compared to predrug value. (b) Antinociceptive effects of DLT were assessed in the ipsilateral and contralateral hind paws of sham (squares) and neuropathic pain (circles) rats on day 14 post-PNI. Saline (30 μl, i.t.; dashed lines) was administered as a control. DLT had no effect on thermal thresholds in the hind paws of sham animals or in the hind paw contralateral to PNI, but significantly increased thermal withdrawal thresholds in the rat hind paw ipsilateral to PNI. Data represent means ± *SEM* for *N* = 7–9 per group. #*p* < 0.05, ##*p* < 0.01 compared to sham-saline. (c) The dose-dependent, acute antinociceptive effects produced by i.t. DLT (i-iii) and morphine (MS) (iv-vi) were evaluated using the hot water tail flick test. Tail flick latencies were measured prior to and every 10 min following drug injection in sham and PNI rats on day 7 post-surgery (ii, v). The percentage of maximum possible effect (% M.P.E.) was calculated at the time of peak antinociception for MS (30 min) and DLT (20 min), and these data were used to plot drug–response relationship curves (i, iv). The antinociceptive time course and area under the curve (A.U.C.) for this time course of antinociception is shown for MS (5 μg; v, vi) and DLT (10 μg, ii, iii). DLT-induced antinociception was enhanced, whereas MS-induced antinociception was attenuated by the presence of NP pain. Data represent means ± *SEM* for *N* = 7–9 per group. **p* < 0.05, ****p* < 0.001 compared to sham surgery control groups

pain-naïve and PNI Sprague Dawley rats. Morphine- and DLT-induced antinociception peaked at 20 and 30 min postinjection, respectively; thus, the % M.P.E. values were calculated at those time points to generate dose–response curves. PNI produced a rightward shift in the morphine dose–response curve (two-way ANOVA revealed an effect of dose ($F_{3, 39}$ = 36.28, **p* < 0.0001) and pain ($F_{1, 39}$ = 5.562, **p* = 0.0235), but no interaction ($F_{3, 39}$ = 0.2388, *p* = 0.8688), which was statistically significant at the 5 μg dose compared to sham animals (*p* = 0.0101; Figure 1c iv). The ED_{50} for morphine in the sham animals was 0.682 (95% CI: 0.314–1.27), whereas the ED_{50} for PNI rats was 1.817 (95% CI: 1.112–2.89). In contrast, the dose–response curve for DLT was shifted to the left in PNI rats compared to sham controls (two-way ANOVA revealed an effect of dose ($F_{3, 47}$ = 3.531, **p* = 0.0218) and pain ($F_{1, 47}$ = 4.913, **p* = 0.0315), but no interaction ($F_{3, 47}$ = 0.3209, *p* = 0.8102), achieving significance at the 10 μg dose (*p* = 0.0234; Figure 1c i). The ED_{50} for DLT in sham animals was 10.97 (95% CI: 6.297–19.64), whereas the ED_{50} for PNI rats was 4.524 (95% CI: 2.575–7.365). Accordingly, the analgesic time-courses were plotted for the 5-μg morphine (Figure 1c v, vi) and 10 μg DLT (Figure 1c ii, iii) doses. Morphine produced significantly less antinociception in PNI rats throughout the 60-min time course (10 min: *p* = 0.0184; 20 min: **p* = 0.0004; 30 min: **p* = 0.0101; 40 min: **p* = 0.0003). However, DLT-mediated antinociceptive effects were enhanced in PNI rats compared with shams (20 min: **p* = 0.0234; 40 min: **p* = 0.0095).

3.2 | Opposing actions of DOR agonism and antagonism on place preference tests in PNI rodents

The effect of drug preference following spinal administration of DLT was assessed using a CPP paradigm in rats. Long-Evans rats were subjected to the CPP protocol beginning 7 days after PNI or sham surgeries, where conditioning began 9 days after pain onset (Figure 2a). The conditioning apparatus was unbiased, as animals spent equal time in both conditioning chambers during the habituation and preconditioning phases (Figure S3). Intrathecal administration of DLT (30 μg) produced a significant CPP in PNI (t_{12} = 2.328, **p* = 0.04), but not in sham (t_{11} = 1.25, *p* = 0.239) animals (Figure 2b). Examples of mouse tracking and heatmaps of time spent in each chamber are presented in Figure 2c.

In order to determine if the CPP produced by the DOR agonist in PNI rats was generalizable to a different rodent species, we preformed similar experiments in C57BL/6J mice. The time course of conditioning following surgery was similar to the rat experiment described above (Figure 2d). Systemic administration of the DOR agonist SNC80 (5 mg/kg, i.p) produced a CPP in PNI (t_{14} = 2.914, **p* = 0.011), but not in sham (t_{16} = 0.860, *p* = 0.402) or pain-naïve mice (t_{20} = 1.353, *p* = 0.1912; Figure 2e).

To determine if endogenous activity at DORs modulates pain unpleasantness, we assessed whether administration of the DOR antagonist naltrindole could produce a CPA in PNI but not in pain-naïve animals. Similar to the experimental protocol described above for DOR agonists (Figure 2f), mice were conditioned to naltrindole (5 mg/kg, i.p.) for 8 days (four drug and four vehicle injections) beginning 9 days after surgery to generate neuropathic pain animals or sham controls. Systemic administration of naltrindole produced a CPA in PNI (t_9 = 2.412, **p* = 0.039), but not in pain-naïve (t_7 = 0.310, *p* = 0.7655) or sham (t_9 = 1.654, *p* = 0.1326) mice. Examples of mouse tracking and heatmaps of time spent in each chamber are presented in Figure 2h.

3.3 | Nerve injury enhances DOR function

To determine the extent to which chronic neuropathic pain alters the functional activity of DORs in the spinal cord of pain-naive and PNI Long-Evans rats, the activation of DORs was quantified by GTPγS autoradiography in the superficial spinal cord 14 days post-PNI. Examples of heat-map autoradiograms of [^{35}S]GTPγS binding are shown in Figure 3a, where warm (red) colors reflect more DLT-stimulated DOR activity and cold (blue) colors indicate less DOR activity. Quantification of radioactivity is presented in Figure 3b. DLT-induced GTPγS binding was increased in the ipsilateral spinal cord of PNI rats, but not in pain-naïve or sham animals. A two-way ANOVA revealed a significant effect of pain ($F_{3, 67}$ = 7.263, **p* = 0.0003), but not of side/laterality ($F_{1, 67}$ = 0.0942, *p* = 0.7598) or interaction ($F_{3, 67}$ = 0.8886, *p* = 004,517). *Post hoc* analysis revealed

a significant effect in the ipsilateral spinal cord (*$p < 0.05$ compared to the pain-naïve group, #$p < 0.05$ compared to the sham group, $ compared to the PNI group without antagonist administration). This increase was blocked by co-incubation of DLT with the DOR antagonist SDM25N. No significant difference was detected between any of the surgical groups on the contralateral side of the spinal cord.

3.4 | *In vivo* Fluo-DLT internalization

Due to the previous criticism of DOR antibodies (Scherrer et al., 2009), we indirectly assessed the change in plasma membrane distribution of DORs following nerve injury via the *in vivo* Fluo-DLT internalization assay. We previously used this technique to visualize

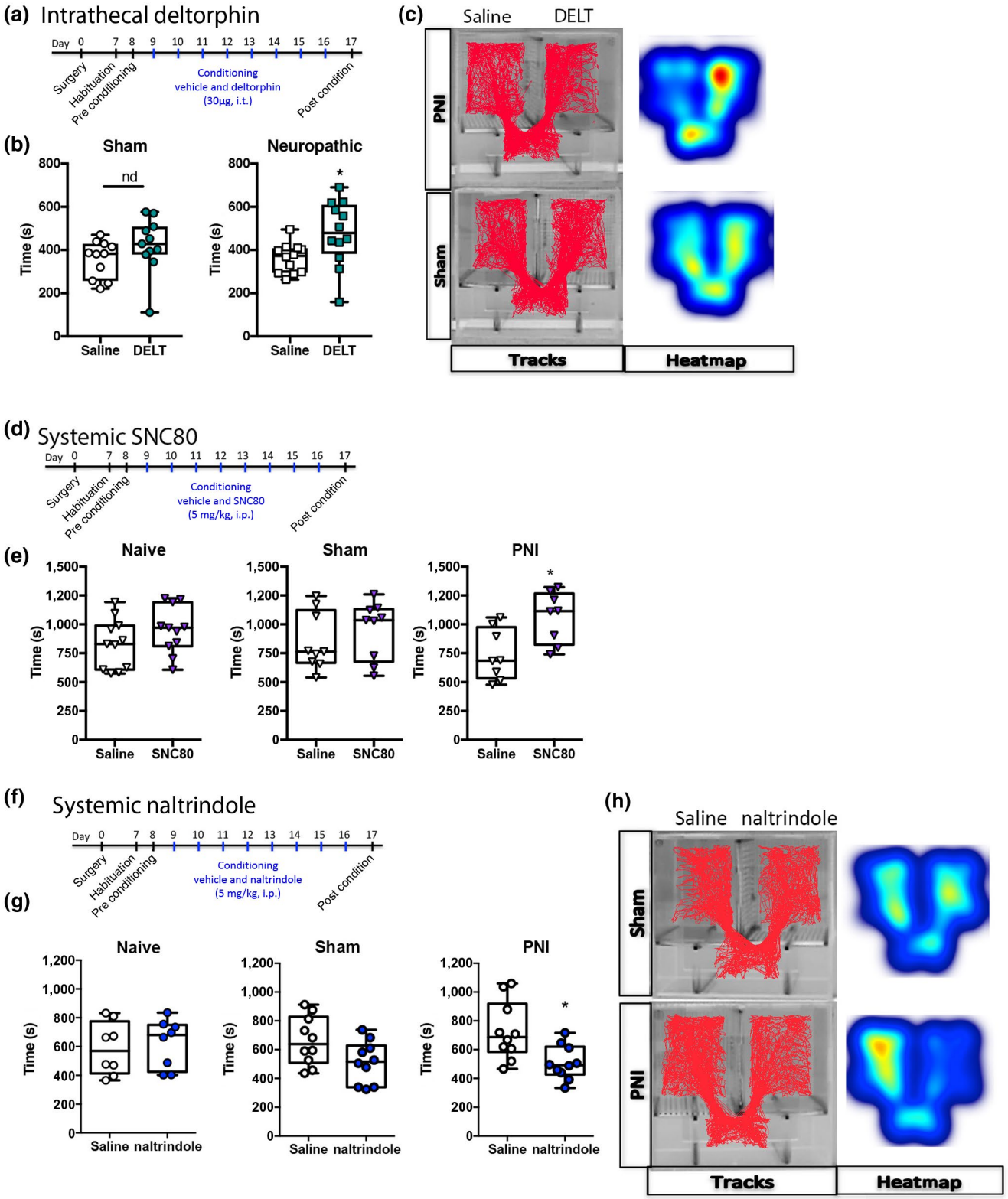

FIGURE 2 Activating delta opioid receptors (DORs) produces negative reinforcement, whereas blocking DORs produces a conditioned place aversion (CPA) in neuropathic pain states. (a) Time course of drug treatment and conditioning in rats. (b) In sham rats: spinal administration of deltorphin (DLT, 30 μg) produced a conditioned place preference (CPP) in rats with neuropathic pain, but not in sham controls. (c) Representative data of activity tracks and heatmaps of DLT CPP. (d) Time course of drug treatment and conditioning in mice (SNC80). (e) Systemic administration of the DOR agonist SNC80 (4-[(*R*)-[(2*S*,5*R*)-4-allyl-2,5-dimethylpiperazin-1-yl](3-methoxyphenyl) methyl]-*N*,*N*-diethylbenzamide; 5 mg/kg, i.p.) did not produce a CPP in pain-naïve or sham control mice; it did, however, produce a significant effect in mice with peripheral nerve injury (PNI). These data suggest that the DOR agonist produces a negative reinforcement (alleviation of a negative stimulus (pain) in the PNI mice. (f) Time course of drug treatment and conditioning in mice (naltrindole). (g) Systemic administration of the DOR antagonist naltrindole (5 mg/kg, i.p.) did not produce a CPP or CPA in pain-naïve or sham control mice, but did produce a significant CPA in mice with PNI, suggesting that tonic activation of DORs modulates ongoing pain in a model of neuropathic pain. (h) Representative data of activity tracks and heatmaps of mice with naltrindole-induced CPA

receptor-mediated internalization of opioid peptides in cultured neurons (Lee, Cahill, Vincent, & Beaudet, 2002) and morphine-induced changes in cell surface DORs in Long-Evans rat spinal cord neurons (Morinville et al., 2004). Intrathecal injection of the highly selective fluorescent DOR agonist, ω-Bodipy red-[D-Ala2]-deltorphin resulted in punctate fluorescent labeling of numerous nerve cell bodies in all layers of the lumbar spinal cord (Figure 3c). The distribution pattern of Fluo-DLT-labeled neurons in the lumbar spinal cord was similar between sham and PNI rats. Greater overall fluorescence levels in laminae IV-V of the dorsal horn, both ipsilateral and contralateral

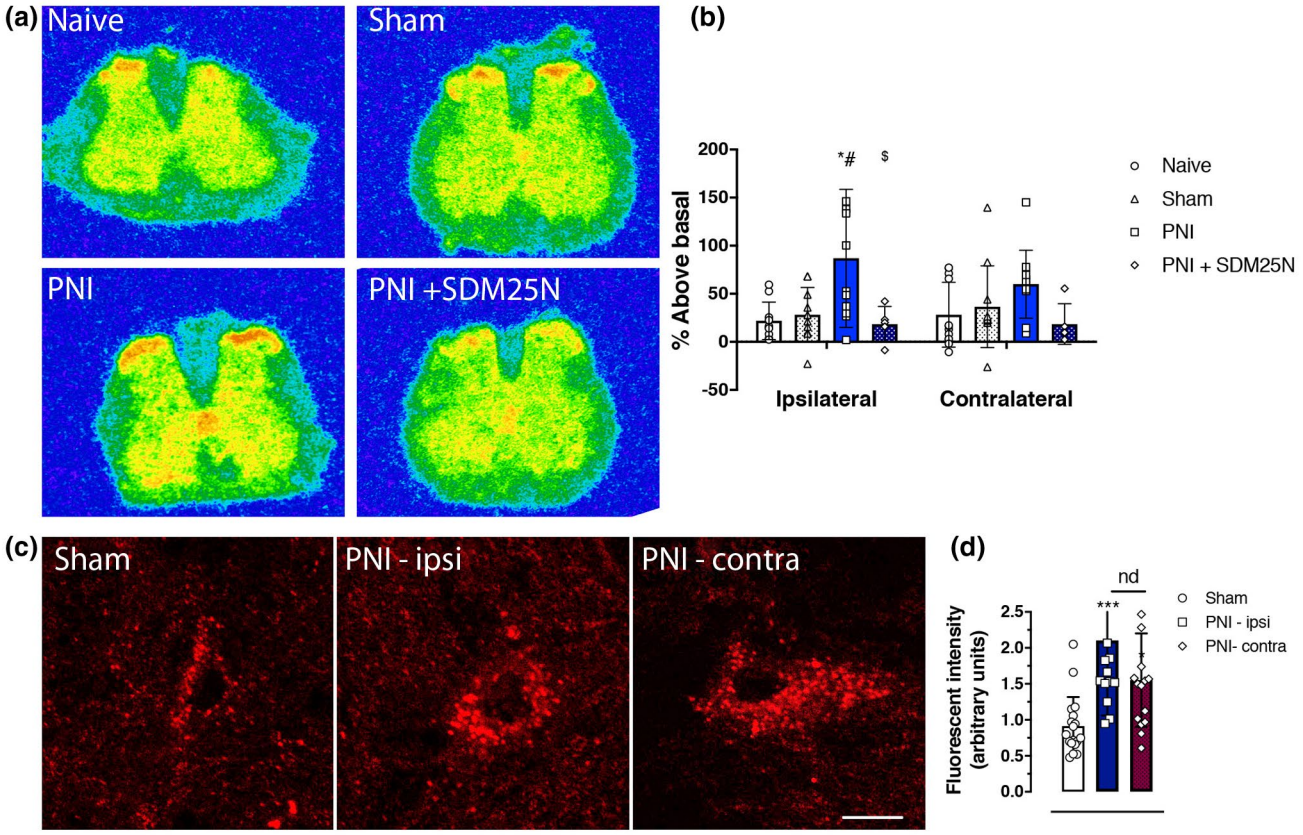

FIGURE 3 Functional upregulation of delta opioid receptors (DORs) in the spinal cord of rats with neuropathic pain. (a) Representative autoradiograms of DOR agonist-induced [^{35}S]GTPγs binding in transverse lumbar spinal cord sections from pain-naïve, sham, and peripheral nerve injury (PNI) rats. (b) Increases in DOR agonist deltorphin (DLT; 1 μM)-stimulated [^{35}S]GTPγs binding are evident in the superficial dorsal spinal cord of PNI mice compared to both pain-naïve and sham controls. This increase in agonist-induced GTP binding was prevented by co-incubation of the DOR antagonist SDM25N (1 μM). (c) High magnification confocal microscopic images of fluorescent-deltorphin (Fluo-DLT)-labeled neurons in the rat dorsal spinal cord 20 min after intrathecal administration of the fluorescent agonist (0.8 nmol). Images are presented in glow scale, where white represents the highest fluorescence intensity and red represents the lowest (black indicates the absence of fluorescent signal). Florescent puncta are evident throughout the perikaryal cytoplasm, where greater fluorescence is evident in spinal cord sections of PNI (14 days post-surgery) compared to sham control rats. Scale bar is 10 μm. (d) Densitometric quantification of fluorescent labeling showing a significant bilateral increase of Fluo-DLT internalization in PNI compared to sham surgery control rats; there was no difference between the ipsilateral and contralateral sides of the dorsal spinal cord of PNI rats

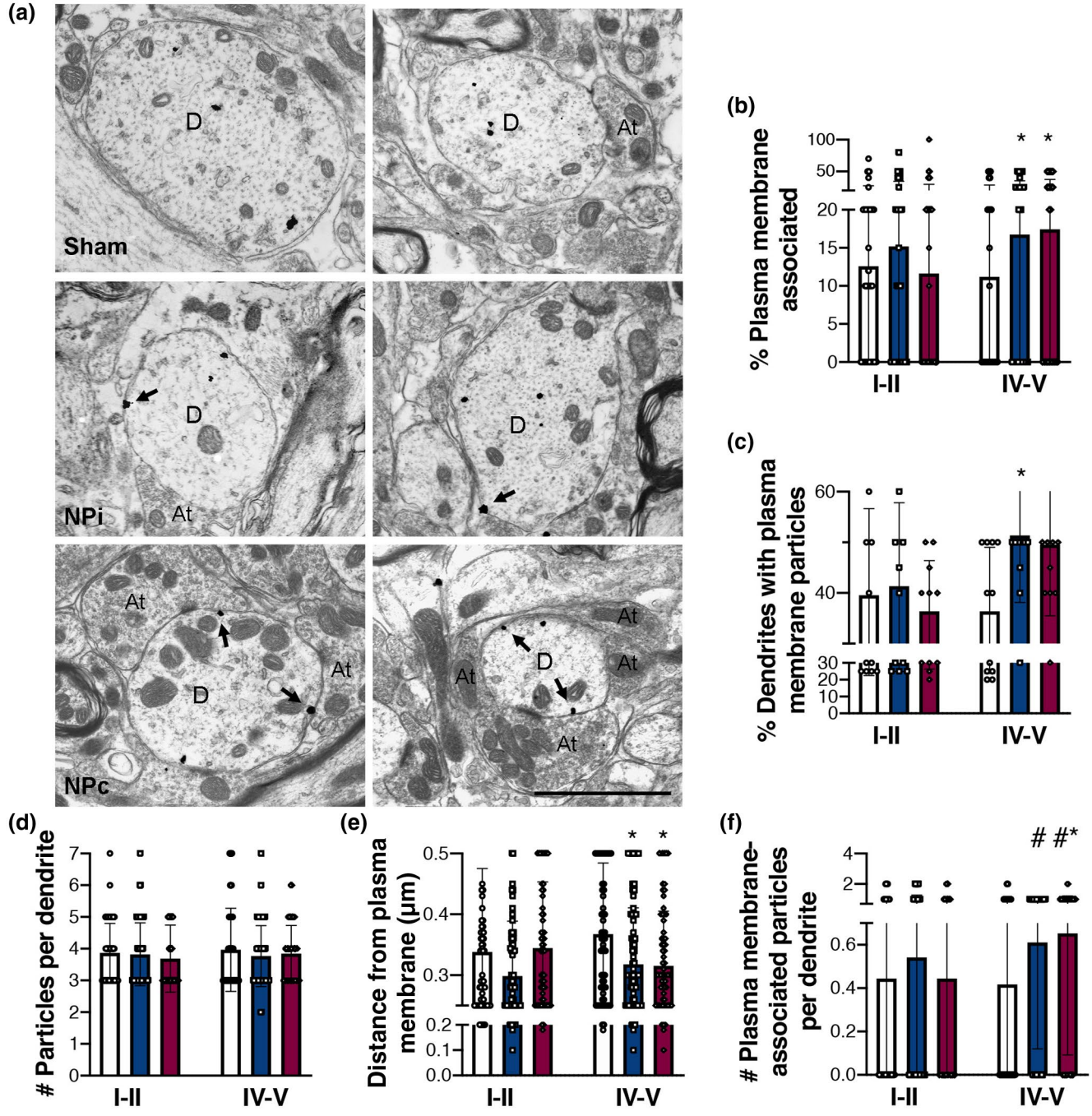

FIGURE 4 Neuropathic (NP) pain changes the subcellular localization of delta opioid receptors (DORs) in the deep dorsal spinal cord, ipsilateral to peripheral nerve injury (PNI). (a) Electron photomicrographs showing the subcellular localization of DOR immunoreactivity within lamina V dendrites from sham and NP pain (NPi: ipsilateral, NPc: contralateral) rats 14 days post-surgery. Silver-intensified gold particle labeling predominantly occurred at intracellular sites in all groups; however, PNI increases cell surface density of DORs on both the ipsilateral and contralateral sides. Arrows indicate gold particles associated with the plasma membrane. D, dendrite; At, axon terminal. Scale bar = 2 µm. (b–f) Quantitative analyses of DOR immunogold labeling in the dorsal spinal cords of sham (white bars) and PNI (blue: ipsilateral; red: contralateral) rats 14 days post-surgery. (b) Percentage of total gold particles associated with the plasma membrane. (c) Average number of plasma membrane-associated gold particles in each dendritic profile. (d) Total number of gold particles counted in each dendritic profile. (e) Average linear distance between gold particles and the nearest point of the plasma membrane. (f) Number of plasma membrane-associated gold particles per dendrite. Roman numerals indicate laminar region from which dendrites were sampled within the dorsal horn. Data represent means ± *SEM* Statistical analyses within each laminar region by one-way ANOVA, followed by Tukey's multiple comparison tests (MCTs), or by two-tailed, un-paired *t*-tests. * $p < 0.05$ compared to shams by Tukey's MCT. $^{\#}p < 0.05$ compared to shams by *t*-test

to PNI, were evident compared with sham control rats (Figure 3d). There was no difference in fluorescence intensity between the ipsilateral and contralateral sides of the spinal cords of PNI animals (Figure 3d).

3.4.1 | Effects of nerve injury on DOR subcellular localization

To determine the effects of PNI on DOR subcellular localization, the distribution of silver-intensified gold particle labeling was assessed in dendritic profiles within the dorsal spinal cords of PNI and sham Sprague Dawley rats. Consistent with previous reports (Cahill, McClellan, et al., 2001; Cahill, Morinville, et al., 2001), some gold particles were detected on plasma membranes; however, the vast majority were intracellularly localized within perikaryal and dendritic profiles, axons and, to a lesser degree, axon terminals (Figure 4a). Some gold particles were observed in association with endoplasmic reticulum, Golgi networks, and mitochondria. The majority of plasma membrane-associated DORs were found at extrasynaptic sites. The membrane perimeters and cross-sectional areas of dendritic profiles sampled from laminae I-II and V are outlined in Table 1. Only dendrites of sizes which completely conformed to the constant region-of-interest boundary on the electron microscope at 15,000× magnification were imaged. Most profiles were of similar size and shape; however, the dendrites sampled from the ipsilateral side of PNI rats (NPi) in laminae I-II were significantly smaller than those sampled from sham rats and the contralateral side of PNI (NPc) rats in the same laminar regions. The smaller size of NPi dendrites yielded artificially high DOR quantitative values (i.e., gold particles per unit length of membrane; particles per unit^2 area), which we felt were more reflective of dendritic size than of real differences in DOR expression. For this reason, DOR expression is normalized and expressed as a "per dendrite" value in the current study. There were no differences in dendritic size among samples from the deep dorsal horn.

Quantitative analyses of DOR ultrastructural distribution revealed a bilateral increase in cell surface expression of gold labeled-DORs in lamina V, but not laminae I-II, dendrites following unilateral PNI. Representative electron photomicrographs from lamina V are displayed in Figure 4a. The percentage of total gold particles associated with the plasma membranes of lamina V profiles from PNI rats (NPi: 16.6%, NPc: 17.4%) was significantly higher than that of sham rats (11.1%; one-way ANOVA, $F_{2, 331} = 3.350$, $p < 0.05$; *t*-test vs. sham: NPi $p < 0.05$, NPc $p < 0.05$; Figure 4a,b). This change translates into 50% and 57% increases in membrane-bound DOR in the ipsilateral and contralateral dorsal horns, respectively. There was no effect of nerve injury on the total number of gold particles counted per dendrite (one-way ANOVA, $p > 0.05$; Figure 4d), indicating that the increase in cell surface expression of DORs was likely a result of redistribution of receptors, rather than increased biosynthesis. The density of DORs on the plasma membrane was similarly higher in PNI rats than in sham rats (one-way ANOVA, Tukey's MCT, sham vs. NPc $p < 0.05$; *t*-test vs. sham: NPi $p < 0.05$, NPc $p < 0.05$; Figure 4c,f). To assess the overall distribution of DORs within dendritic profiles, the linear distance of each gold particle from the plasma membrane was measured. The distance was significantly shorter in the PNI rats compared with shams (one-way ANOVA, $F_{2, 1,280} = 3.078$, $p < 0.05$; *t*-test vs. sham: NPi $p < 0.05$, NPc $p < 0.05$ (Figure 4e), suggesting an overall mobilization of DORs from intracellular compartments toward the plasma membrane following nerve injury. Finally, the percentage of sampled dendrites that expressed two or more gold particles on the cell surface was calculated. In sham rats, 36.0% of dendrites expressed DOR on the plasma membrane. Following PNI, this population increased significantly to 51.2% in the ipsilateral dorsal horn (one-way ANOVA, Tukey's MCT, $F_{2, 24} = 9.488$, sham vs. NPi $^*p < 0.05$). The percentage of such dendrites in the contralateral spinal cord of PNI rats also increased (49.8%); however, this value failed to reach significance. PNI did not produce any changes in DOR subcellular distribution within laminae I-II dendrites on either side of the spinal cord, as assessed by analyses identical to those outlined above (Figures 4 and S4).

TABLE 1 Details of immunolabeled dendritic profiles sampled in each experimental group

Condition	Total number of dendritic profiles sampled	Average dendritic perimeter (μm)	Average dendritic cross-sectional area (μm^2)
SHAMi			
I,II	85	9.39 ± 0.305	3.60 ± 0.208*
V	99	10.57 ± 0.263	4.14 ± 0.196
NPi			
I,II	132	8.76 ± 0.251	3.00 ± 0.159
V	133	10.05 ± 0.219	3.97 ± 0.174
NPc			
I,II	88	9.99 ± 0.255**	3.87 ± 0.179**
V	102	10.50 ± 0.259	4.35 ± 0.197

Note: Roman numerals indicate laminar region from which dendrites were sampled within the dorsal horn. Statistical analyses between values within a laminar region were performed by one-way ANOVA, Bonferroni MCT. Asterisks denote significant difference from NPi laminae I,II; $^*p < 0.05$, $^{**}p < 0.01$.

Abbreviations: NPc, neuropathic contralateral; NPi, neuropathic ipsilateral; SHAMi, sham ipsilateral.

3.5 | Basal and capsaicin-evoked CGRP release

There has been conflicting reports whether chronic pain alters the function of presynaptic DORs on primary afferent neurons. While many peptides in the spinal cord can arise from descending neurons or are present within spinal cord interneurons, CGRP content in the spinal cord arises solely from primary afferent terminals, allowing us to directly assess the extent chronic pain modulates DOR function on these terminals. In the absence of stimulation, CGRP was detected in the superfusate collected from spinal cords slices of sham and PNI Long-Evans rats (Figure 5a). Basal release of CGRP was similar between the ipsilateral and contralateral sides of the dorsal spinal cord of sham rats. Additionally, basal release of CGRP from the contralateral dorsal spinal cord of PNI rats was not significantly different than that of sham control rats. However, basal release of CGRP from PNI rats was significantly increased compared to all other groups ($F_{(3,21)}$ = 9.393, p < 0.001). The addition of 100 μM capsaicin to the perfusion buffer to depolarize primary afferent neurons releasing neuropeptides increased CGRP release above basal levels in spinal cord slices for both pain-naive ($F_{(3,24)}$ = 50.18, p < 0.0001) and PNI ($F_{(3,24)}$ = 47.09, p < 0.0001) rats (Figure 5b). The evoked release from the ipsilateral spinal cord slices of PNI rats was significantly greater than that from sham control slices (t_{10} = 5.770, p = 0.0002). When DLT was added to the perfusate with capsaicin, the DOR agonist significantly attenuated capsaicin-evoked release in tissue from both sham and PNI rats. The percent inhibition induced by the DOR agonist was significantly higher in the PNI compared to naive group (t_{10} = 2.346, p = 0.0409, Figure 5b).

3.6 | Neonatal capsaicin experiments

The mechanisms underlying nerve injury-induced changes in DOR function are unclear. Previous studies have shown that augmented DOR function are due to increased receptor trafficking within primary sensory afferent neurons (Morinville et al., 2004). Thus, we investigated the role of capsaicin-sensitive afferents in the DOR functional competence following nerve injury by neonatal treatment with capsaicin, which leads to selective destruction of unmyelinated C fibres (Scadding, 1980). Immunohistochemical techniques were used to visualize changes nociceptive molecular markers in the dorsal horn. The antinociceptive effects of spinal DLT were examined in these animals using the hot water tail flick test.

3.7 | General observations of rats treated with capsaicin

3.7.1 | Neonatal injections

Upon injection with capsaicin, Sprague Dawley rat pups generally vocalized and writhed for a few minutes, and often exhibited mild respiratory depression requiring administration of oxygen to stimulate breathing. This reaction typically proceeded for 10 to 15 min postinjection, after which pups appeared normal. No such reaction was observed in pups treated with vehicle. In both groups, the dam received the pups normally following injections.

3.7.2 | Effects of neonatal capsaicin on general health of adult rats

Vehicle-treated Sprague Dawley rats were indistinguishable from untreated controls. Capsaicin-treated rats developed cutaneous lesions on the head and neck area, likely, in part, as a result of trophic disturbances (Carrillo et al., 1998; Thomas, Dubner, & Ruda, 1994). Otherwise, capsaicin produced no observable changes in indicators of overall health, such as growth rate, as assessed by weekly measurements of body mass (data not shown).

3.8 | Effects of nerve injury and neonatal capsaicin treatment on expression of primary afferent and nociceptive markers: IB4, substance P, and CGRP

3.8.1 | IB4

Spinal IB4 immunoreactivity (IR) was observed most intensely in inner lamina II within the dorsal gray matter of vehicle-treated pain-naïve rats (Figure 5c). Some labeling was also evident in white matter regions, likely corresponding to the path of incoming afferent fibers. Mean density values were compared between groups for the ipsilateral ($F_{3, 44}$ = 60.92, p < 0.0001) and contralateral ($F_{3, 44}$ = 63.41, p < 0.0001) dorsal horn regions (Figure 5c). Following PNI, a substantial bilateral reduction in IB4-IR (~26% and ~22% in the ipsilateral and contralateral sides of the spinal cord, respectively) was observed, which was most apparent in the medial region of inner lamina II (ipsi: p < 0.001; contra: p < 0.001). Neonatal capsaicin treatment decreased spinal IB4-IR by ~53% compared with vehicle-treated pain-naïve rats (p < 0.001). This decrease was observed throughout inner lamina II and was particularly evident in the lateral region. PNI did not produce any further decrease in IB4-IR in capsaicin-treated rats.

3.8.2 | SP

Spinal SP-IR was evident in laminae I and II, with some white matter labeling presumably corresponding to incoming afferent fibers, which terminate in the deeper dorsal horn where sparse axonal SP-IR was present (Figure 5c). PNI did not produce an observable change in SP-IR labeling. Neonatal treatment with capsaicin produced a significant reduction in SP-IR (~26%) in the dorsal horn (ipsi: $F_{3, 44}$ = 6.511, p < 0.05; contra: $F_{3, 44}$ = 7.888, p < 0.05). PNI did not alter SP-IR labeling in capsaicin-treated rats.

3.8.3 | CGRP

Spinal CGRP-IR was observed primarily in lamina I and outer lamina II, with some labeled axons traversing into deeper dorsal horn laminae (Figure 5c). PNI produced no significant effect on CGRP-IR in either the ipsilateral or contralateral side of the dorsal horn (Figure 5c). Neonatal capsaicin treatment significantly reduced CGRP-IR (~40%) in the superficial dorsal horn (ipsi: $F_{3,28} = 6.407$, $p < 0.005$; contra: $F_{3,28} = 16.60$, $p < 0.001$) and abolished CGRP-IR axonal labeling in deeper laminae. PNI produced no change in CGRP-IR in capsaicin-treated animals.

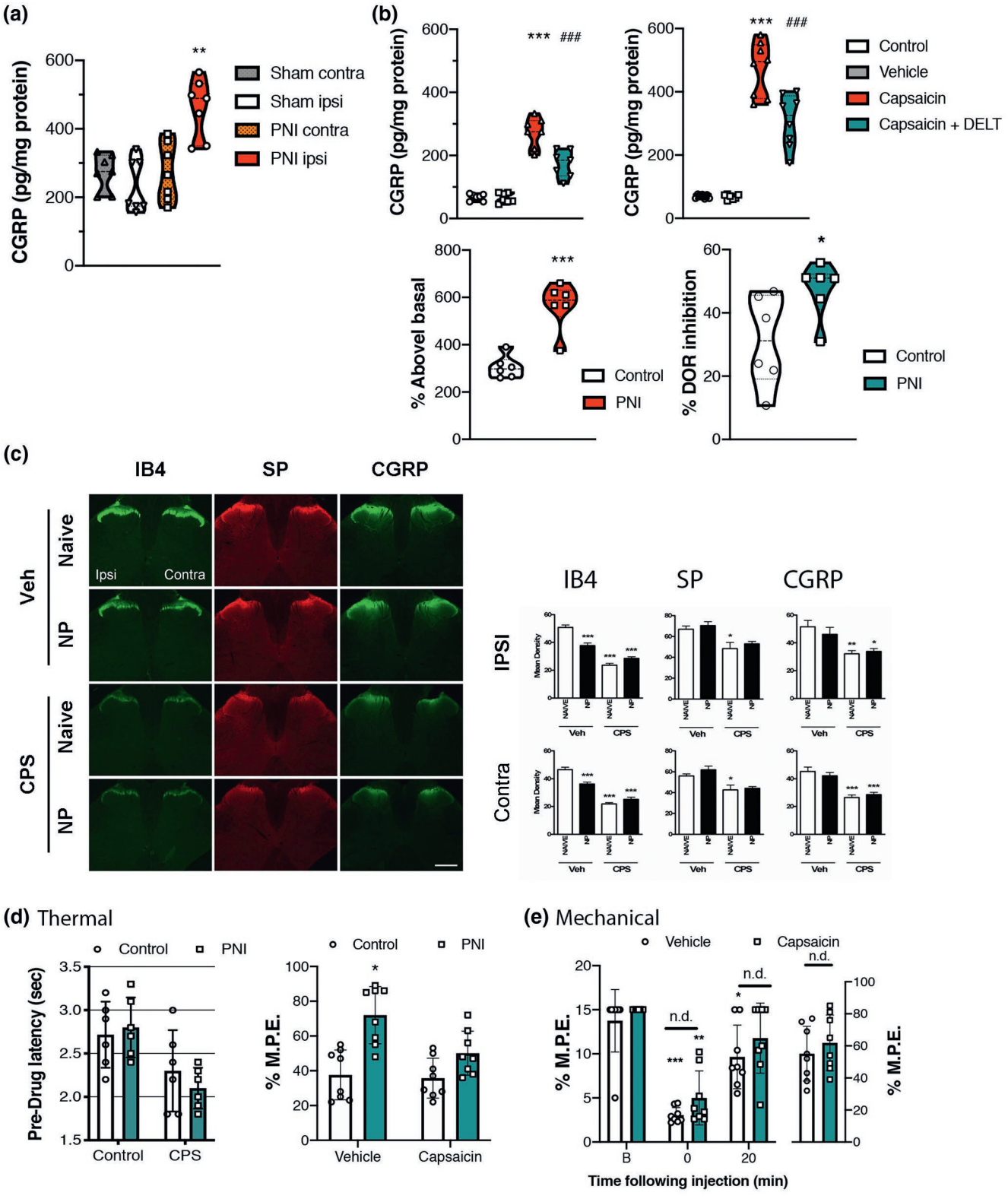

FIGURE 5 Effects of delta opioid receptor (DOR) agonists on calcitonin gene-related peptide (CGRP) release and pain hypersensitivities following neonatal capsaicin administration. (a) Basal concentrations of CGRP were increased in spinal cord slices from rats with peripheral nerve injury (PNI) on the dorsal ipsilateral compared to the contralateral side, and compared to sham animals. (b) Capsaicin increased release of CGRP in both sham and PNI rats, which was reduced by co-incubation with deltorphin (DLT). The percent of evoked release was significantly higher in PNI compared to naïve tissue. Additionally, the inhibition of evoked release induced by DLT was significantly greater in tissue from PNI compared to pain-naive rats. Data represent means ± *SEM* for $N = 6–9$ per group. $^{*}p < 0.05$, $^{*}p < 0.001$. (c) The effects of neonatal capsaicin treatment on nociceptive afferent markers were assessed in lumbar spinal cords of adult pain-naïve and PNI rats by fluorescent immunohistochemistry on day 7 post-surgery. Representative low-magnification photomicrographs of isolectin B4 (IB4)-, CGRP-, and substance P (SP)-immunoreactive labeling. The left side is ipsilateral to the site of nerve injury. Scale bar = 1 mm, which applies to all. Mean intensity of immunoreactive labeling was quantified in the ipsilateral (upper panel) and contralateral (lower panel) dorsal horn regions. Data represent means ± *SEM* for four sections per rat and $n = 7–9$ rats per condition. Statistical analyses by one-way ANOVA, followed by Bonferroni's *post hoc* multiple comparisons test (MCT). $^{*}p < 0.05$; $^{**}p < 0.01$; $^{***}p < 0.001$ compared to vehicle-treated, pain-naïve rats. (d) The effects of neonatal capsaicin treatment on DOR-mediated antinociception in the hot water tail flick test in adult pain-naïve and PNI rats 7 days post-surgery. The left panel compares predrug withdrawal latencies. There was no significant difference in thermal thresholds in capsaicin-treated compared to control rats. The right panel shows the percentage of maximum possible effect (% M.P.E.) at 20 min following intrathecal injection of 10 μg of DLT. Statistical analyses by two-tailed, unpaired *t*-test versus vehicle-treated pain-naïve rats ($^{*}p < 0.05$). (e) Mechanical withdrawal responses were assessed 14 days post-surgery using calibrated von Frey filaments in PNI rats treated neonatally with capsaicin (green bars) or not (white bars). The response pattern was used to calculate the 50% paw withdrawal threshold (50% P.W.T.) The anti-allodynic effects of 10 μg of DLT were assessed 20 min postinjection. Statistical analyses by two-tailed, unpaired *t*-test versus vehicle-treated pain-naïve rats ($^{*}p < 0.05$). CPS, capsaicin-treated; Veh, dimethyl sulfoxide (DMSO) vehicle-treated

3.9 | Effects of neonatal capsaicin treatment on nerve injury-induced changes in DOR agonist effects

3.9.1 | Acute thermal pain testing

PNI did not produce thermal hypersensitivity in vehicle-treated Sprague Dawley rats, as hot water tail flick latencies were similar to vehicle-treated controls (Figure 5d). Furthermore, neonatal capsaicin treatment did not alter baseline thermal nociception in pain-naïve or PNI rats. The antinociceptive effects of spinally administered DLT were similar in vehicle- and capsaicin-treated pain-naïve rats (Figure 5d, white bars), indicating that capsaicin treatment did not alter DOR agonist activity in control rats. In vehicle-treated rats, PNI produced a significant increase in DLT-mediated antinociception (unpaired *t*-test, $p = 0.0188$), consistent with data presented in Figure 1, but this increase was absent in PNI rats that received capsaicin as neonates, suggesting a role for capsaicin-sensitive primary afferents in the PNI-induced changes in DOR function that regulate thermal nociception.

3.9.2 | Innocuous mechanical stimulus testing

Prior to surgery, all Sprague Dawley rats were unresponsive up to the maximum tactile force of 15 g. At 14 days post-surgery, untreated rats displayed tactile allodynia in the ipsilateral hind paw ($F_{2, 18} = 22.34$, $p < 0.001$), which was reversed by intrathecal injection of DLT (10 μg; Figure 5e). Similarly, capsaicin-treated PNI rats displayed a significant decrease in mechanical withdrawal thresholds in the ipsilateral hind paw on day 14 post-surgery, indicative of tactile allodynia ($F_{2, 14} = 10.77$, $p < 0.01$). No such sensitivity was evident in the contralateral paw (data not shown). Furthermore, intrathecal DLT (10 μg) administration attenuated this hypersensitivity, restoring withdrawal thresholds to values not different from baseline thresholds. Withdrawal thresholds and % M.P.E. values were similar between untreated and capsaicin-treated rats, indicating that neonatal capsaicin treatment altered neither the PNI-induced development of tactile allodynia nor the anti-allodynic effects of DLT, unlike the effects of capsaicin on thermal antinociception produced by the DOR agonist.

4 | DISCUSSION

The major novel findings of this study are that PNI-induced neuropathic pain causes an upregulation of DOR function in the dorsal spinal cord that is evidenced by (a) delta agonist-induced place preference in both chronic pain but not in pain-naïve mice and rats, indicative of the expression of negative reinforcement. (b) Our data suggest that PNI engaged the endogenous DOR system to dampen pain unpleasantness, as blocking DORs produced a CPA in PNI rats, but not in control animals. (c) We present two pieces of evidence based on the internalization induced by a fluorescent DOR ligand and immunogold electron microscopy, suggesting that one of the most parsimonious explanations for the increase in DOR function in chronic neuropathic pain is due to an increase in cell surface expression of DORs in spinal dorsal horn neurons, primarily within deeper laminae, rather than superficial laminae of the dorsal horn. (d) An increase in G protein activation, as determined by GTPγS autoradiography. (e) Finally, we showed mechanistic data supporting a role for DOR expression on primary afferent neurons in the modality-specific regulation of nociception. Hence, eliminating DORs in primary afferent sensory neurons via capsaicin administration in neonates prevented the enhanced function of DOR agonists observed in the thermal nociceptive tests, without affecting DOR agonist

modulation of mechanical nociception. These results complement our behavioral data where we show that there is an increase in effectiveness of the ability of DOR agonists to attenuate both thermal and mechanical nociception associated with nerve pain. Additionally, unlike the observed rightward shift of morphine-induced antinociception in PNI rats, DOR agonist-induced antinociception was enhanced in the thermal tail flick test.

4.1 | Pain sensation and unpleasantness is modulated by DOR activation

Unilateral PNI produced thermal and mechanical hypersensitivity in the ipsilateral hind paw, as indicated by a significant reduction in withdrawal latencies in response to noxious heat and the application of von Frey filaments. The anti-hyperalgesic and anti-allodynic effects of DOR agonists observed in PNI rats in the current study are in accordance with previous reports that DOR agonists alleviated nerve injury-induced hypersensitivities to noxious thermal and innocuous mechanical stimuli following peripheral, spinal, or supraspinal administration (Cahill, Holdridge, & Morinville, 2007). Antinociceptive effects of DOR agonists were also observed in the contralateral paws of PNI rats, but were completely absent in sham rats. This contralateral change in function has previously been reported, whereby Stewart and Hammond showed that spinal and supraspinal administration of DLT attenuated thermal hyperalgesia induced by peripheral inflammation, and increases in paw withdrawal latencies were observed not only in the injured paw, but also in the uninflamed paw (Hurley & Hammond, 2000; Stewart & Hammond, 1994).

Given that pain is a multidimensional experience and that the negative affect, or how much the pain is "bothersome," has been argued to be a greater metric of quality of life than its sensory component (https://acrabstracts.org/abstract/emotional-pain-and-catastrophizing-infuence-quality-of-life-in-fibromyalgia/), we asked whether DOR agonists may produce a CPP in neuropathic pain but not in control surgery animals. The expression of a CPP in pain, but not "pain-naïve," states is thought to represent a type of negative reinforcement (i.e., animals associate drug effects with alleviation of the ongoing painful experience). Our data demonstrate that DOR agonists do not produce a CPP in control surgery rats or mice, but do elicit a CPP (negative reinforcement) following PNI. Previous studies have reported conflicting evidence of whether DOR agonists produce a CPP (Bals-Kubik, Shippenberg, & Herz, 1990) in otherwise drug- or pain-naïve rodents, with some showing no CPP (Conibear et al., 2020; Hutcheson et al., 2001; Mitchell, Margolis, Coker, Allen, & Fields, 2014). However, one could argue that any study assessing the effects of DOR agonists in a CPP paradigm whereby rodents have undergone surgery to implant long-term, indwelling catheters for repeated drug delivery may induce a stress response sufficient to elicit DOR agonist-induced negative reinforcement. Indeed, DOR activation is suggested to have a role in stress resilience (Henry, Gendron, Tremblay, & Drolet, 2017) and the modulation of mood and emotion (Dripps & Jutkiewicz, 2018; Lutz & Kieffer, 2013), including the associated stress (Connelly & Unterwald, 2019) and anxiogenic effects (Ambrose-Lanci, Sterling, & Bockstaele, 2010) associated with cocaine withdrawal. DOR agonists have also been shown to block place aversion associated with nitroglycerin administration in an animal mode of migraine pain (Pradhan, Smith, Zyuzin, & Charles, 2014).

Another interesting and novel finding in our study was that naltrindole produced a place aversion in pain but not in pain-naive animals. This result suggests that the endogenous opioid system is engaged in chronic pain states and contributes to modulating the pain experience. Our studies do not address the mechanism or circuits underlying this effect and while our data suggest that the negative reinforcement is due to actions at the spinal level (i.e., we report a CPP with intrathecal administration of a DOR agonist), we cannot rule out the possibility of supraspinal actions. For example, DOR plays a protective role in limiting nociceptive and affective manifestations of neuropathic pain due to its expression in forebrain regions. Conditional knockout of DORs from forebrain GABAergic neurons demonstrated enhanced heat hyperalgesia and augmentation of anxiogenic effects in the elevated plus maze, light-dark box test, and forced swim test (Martinez-Navarro et al., 2019). Although this is somewhat contradictory of a previous report in pain-naive mice, this same DOR conditional knockout produced lower levels of anxiety-related behavior (Chung et al., 2015). Future research is needed to understand the contribution of various neuronal circuits in modulating the negative affect associated with DOR activation.

Previous studies have shown that thermal and mechanical hypersensitivities were significantly enhanced in DOR null mutant mice in models of neuropathic and inflammatory pain, supporting the concept that activation or endogenous engagement of the DOR system modulates both the sensory and affective dimensions of pain processing (Gaveriaux-Ruff et al., 2011; Nadal, Banos, Kieffer, & Maldonado, 2006). Although acute nociception is not affected by DOR gene deletion in the absence of ongoing pain, Hao, Yu, and Xu (1998) reported that DOR antagonism by naltrindole enhanced neuropathic pain behaviors in rats with ischemic spinal cord injuries, without affecting nociceptive thresholds in uninjured rats. The neuronal DOR expression that has been shown to modulate various components of ongoing pain has been reported using conditional knockout mice. Thus, ablation of DORs from Nav 1.8 sodium channel subtype-expressing sensory neurons augmented mechanical allodynia, but not thermal hyperalgesia, in both inflammatory and neuropathic (NP) pain models, while mutant mice exhibited normal sensory thresholds to mechanical and thermal stimuli in sham-injured animals (Gaveriaux-Ruff et al., 2011). Although it is possible that Cre expression in dorsal root ganglia in the Nav1.8-Cre mice may not be restricted to nociceptors and may also affect low-threshold mechanoreceptor sensory neurons (Shields et al., 2012), it remains unclear whether deletion of DORs solely on nociceptors is responsible for the enhancement of mechanical pain. It was argued that DORs expressed on myelinated mechanoreceptors are responsible for DOR agonist-induced modulation of mechanical allodynia associated with tissue or nerve injury (Bardoni et al., 2014). We used a neonatal capsaicin treatment approach to destroy primary

afferent neurons, and our spinal cord analysis showed reductions in both peptidergic and non-peptidergic, as well as myelinated, afferent terminals in the spinal cord. This is consistent with previous studies showing that such treatment produces an 80%–90% reduction in C-fibers (Thomas et al., 1994), where a significant expression of transient receptor potential vanilloid receptor 1 was identified in peptidergic and non-peptidergic C-fibers (Hjerling-Leffler, Alqatari, Ernfors, & Koltzenburg, 2007), but also in sympathetic ganglia in neonatal animals (McDougal, Yuan, Dargar, & Johnson, 1983), so it impossible to rule out what influence sympathetic atrophy may have in the development of pain hypersensitivities. We also showed that capsaicin-evoked release of CGRP from spinal cord slices was enhanced in PNI animals compared to sham controls, and the ability of DOR agonists to block this evoked release was enhanced in tissue from PNI animals compared to spinal cord sections of shams. This is consistent with previous reports that DOR agonists can reduce CGRP release (Overland et al., 2009). These data suggest that there is enhanced presynaptic DOR function in nociceptive neurons that allows for modulation of pain hypersensitivities associated with injury, although DOR and CGRP were shown to also be co-expressed in large-diameter neurofilament 200-positive (NF200+) dorsal root ganglia neurons, and DOR agonists inhibited voltage-gated calcium channels in these cells (Bardoni et al., 2014), suggesting the possible neuronal involvement of non-peptidergic primary afferents. Importantly, our result that neonatal capsaicin blocked the enhanced anti-hyperalgesic effect of DOR in thermal, but not in mechanical, testing modalities is intriguing. We suggest that while it is possible that DOR agonists modulate low-threshold primary afferent mechanoreceptors, it is likely that DOR agonists produce their inhibitory effects on mechanical allodynia via activation of DORs expressed in deep laminae of the dorsal horn of spinal cord neurons. This is based on our data demonstrating that DOR cell surface expression increased in deeper dorsal horn neurons, and previous studies reported that DOR expression on somatostatin-positive dorsal horn neurons regulated mechanical nociception (Wang et al., 2018).

4.2 | Nerve injury-induced changes in DOR subcellular distribution

The mechanisms underlying DOR functional enhancement following nerve injury are unclear and do not appear to involve increased receptor synthesis, and we hypothesize that the increase in DOR analgesic effects is due to a change in subcellular localization as we have previously reported in other pain models (Cahill et al., 2007; Cahill, Morinville, Hoffert, O'Donnell, & Beaudet, 2003; Gendron et al., 2016). We thus decided to assess the effects of PNI on subcellular DOR distribution within lumbar spinal cord neurons using immunogold electron microscopy. We examined DOR expression in two dorsal horn regions that act as important relay sites in the processing of nociceptive information: laminae I-II and V. The superficial dorsal horn is the major point of termination of most unmyelinated peptidergic and non-peptidergic C fibers, as well as thinly myelinated Aδ fibers, while the deeper laminae of the dorsal horn receive afferent inputs from large myelinated Aβ, Aδ, and peptidergic C fibers (Ribeiro-da-Silva & De Koninck, 2008). In the current study, some DOR labeling was evident in axons and axon terminals, while a larger proportion was observed in association with neuronal perikarya and dendrites. In all neuronal profiles, DORs were localized, predominantly, in intracellular sites, with very few receptors located on the plasma membrane under basal conditions. This is consistent with all previous ultrastructural immunogold data and with the current behavioral observation that DLT produced no antinociceptive effects in sham-operated rats. PNI produced no change in total expression or subcellular distribution of DORs within laminae I-II dendrites. In contrast, DOR cell surface expression increased by 50% within lamina V dendrites, and this effect was observed on both sides of the spinal cord. This increase did not correlate with any change in the average number of DORs expressed per dendrite, and, therefore, reflects a redistribution of existing DORs from intracellular sites toward the plasma membrane. Postsynaptic profiles in this region mainly represent intrinsic interneurons (Ribeiro-da-Silva & De Koninck, 2008), as well as projection neurons, of the spinothalamic and dorsal column-medial lemniscus ascending tracts (Willis & Coggeshall, 1991). Accordingly, DORs expressed along these tracts are well situated to modulate the transmission of nociceptive inputs, and their recruitment to the cell membrane following nerve injury could underlie the enhanced antinociceptive effects of DLT in PNI rats. While laminae I-II neurons respond chiefly to synaptic communication from peripheral nociceptors, lamina V neurons also receive both direct and indirect nociceptive and non-nociceptive inputs from the periphery, and synapse extensively with neurons of the substantia gelatinosa via antenna-like dorsal dendritic projections. Whereas some lamina V spinothalamic tract cells are selectively responsive to innocuous mechanical, noxious mechanical, or thermal stimuli, other cells—the aptly named wide dynamic range (WDR) neurons—respond to a variety of low- and high-threshold inputs (Willis, 1985), and may serve to integrate afferent inputs from the entire sensory spectrum. Additionally, lamina V spinothalamic tract neurons display "wind up" activity in response to repetitive stimulation from C-fiber inputs. Thus, WDR neurons may contribute to the hypersensitivity and multimodal symptoms of NP pain (Chu, Faltynek, Jarvis, & McGaraughty, 2004; Pertovaara, Kontinen, & Kalso, 1997; Sotgiu, Valente, Caramenti, & Biella, 2006). Interestingly, while prolonged morphine treatment resulted in DOR trafficking throughout the spinal dorsal horn (Cahill, Morinville, et al., 2001; Morinville et al., 2004), the changes in DOR expression and function induced by complete Freund's adjuvant injection (Cahill et al., 2003) and dorsal rhizotomy (Morinville et al., 2004) were most pronounced in lamina V, suggesting an important role of DOR within this laminar region in modulating nociception following a PNI.

Indeed, we observed a shift in compartmentalization, which produced a 50% increase in DOR cell surface expression; however, some pertinent questions remain: What is the large remaining pool of intracellular DORs doing inside the cell? What function are these DORs carrying out? Surely the fate of these receptors in the absence of a definitive physiological stressor or injury is not merely

to sit idle and await degradation. In actuality, the current ultrastructural data likely represent static "snap shots" of what is actually a highly dynamic regulatory mechanism at work. Cell surface trafficking of DORs can be initiated by numerous *in vitro* and *in vivo* stimuli (Cahill et al., 2007; Mittal et al., 2013). The molecular mechanisms underlying these trafficking events have been partially elucidated. For example, they may entail regulation of molecular chaperones or accessory proteins which facilitate G protein-coupled receptor transport, including the arrestins, Homer proteins, and receptor activity-modifying proteins, among many others (Drake, Shenoy, & Lefkowitz, 2006; Mittal et al., 2013). More recently, others have implicated a role for G protein-coupled receptor kinase 2 (GRK2) in reducing the function of cell surface DORs whereby incubation with an inflammatory agent such as bradykinin stimulated the separation of GRK2 away from the DOR, allowing it to become available for receptor activity (Brackley, Gomez, Akopian, Henry, & Jeske, 2016). Further studies will be necessary to investigate the mechanisms involved in nerve injury-induced DOR translocation.

5 | CONCLUSION

In the current study, we demonstrated that intrathecal administration of DOR agonists attenuated nerve injury-induced pain hypersensitivities in the ipsilateral hind paw, exhibiting enhanced dose-dependent effects in the testing of thermal nociceptive modalities. We also showed that PNI altered the endogenous DOR system to mitigate pain associated with nerve injury, and blocking this system increased aversive states. Our data show an outward mobilization of DORs in spinal cord neurons following nerve injury, thus increasing cell surface expression and ligand accessibility; this trafficking event may underlie the enhancement of DOR agonist effects. Together, our data provide strong evidence for both spinal and supraspinal regulation of pain by the DOR system.

DECLARATION OF TRANSPARENCY

The authors affirm that in accordance with the policies set by the *Journal of Neuroscience Research* this manuscript presents an accurate and transparent account of the study being reported and that all critical details describing the methods and results are present.

ACKNOWLEDGMENTS

This work was supported by a generous gift from Ms. Shirley Hatos to C.M.C., start-up funds from University of California, Irvine (C.M.C.), the Shirley and Stefan Hatos Foundation (C.M.C.), the Canadian Institutes of Health Research (C.M.C., M.C.O. MOP 123298), the Canada Research Chairs Program (C.M.C.), the J.P. Bickell Foundation (C.M.C), the Ontario Innovation Trust / Canadian Foundation for Innovation (C.M.C), and the NIH-National Institute of Drug Abuse Grant numbers R01DA041781 (CMC), 1UG3TR003148-01 (CMC) and 2P50 DA005010 (CMC), and the Department of Defense Grant number W81XWH-15-1-0435 (CMC). S.V.H. was funded by an Ontario Graduate Scholarship in Science & Technology. S.L. was supported by a UCI Graduate Division Public Impact Fellowship and a School of Medicine Outstanding Student Fellowship. P.G. was funded by an NSERC postgraduate scholarship. The authors thank Dr. Michael Kawaja for his assistance with spinal cord sectioning and Mariette Lavallee for her technical assistance in ultrathin sectioning.

CONFLICT OF INTEREST

The authors declare they have no conflict of interest and nothing to declare.

AUTHOR CONTRIBUTIONS

All the authors had full access to all the data in the study and take responsibility for the integrity of the data and the accuracy of the data analysis. *Conceptualization*, C.M.C., S.H., and M.C.O.; *Methodology and Data Curation*, C.M.C., S.V.H., S.L., L.X., C.M., and A.S.; *Formal Analysis*, C.M.C., S.V.H., S.L., L.X., C.M., E.O., P.G., A.S., and M.C.O.; *Writing – Original Draft*, C.M.C., S.V.H., E.O., P.G., and M.C.O.; *Writing – Reviewing & Editing*, C.M.C.; *Supervision*, C.M.C. and M.C.O.; *Funding Acquisition*, C.M.C., M.C.O., S.V.H., S.L., and P.G.; *Visualization*, C.M.C., S.V.H., and P.G.

DATA AVAILABILITY STATEMENT

The data that support the findings of this study are available from the corresponding author upon reasonable request.

ORCID

Catherine M. Cahill https://orcid.org/0000-0001-6936-5524
Edmund Ong https://orcid.org/0000-0003-0394-4608
Mary C. Olmstead https://orcid.org/0000-0003-2249-4411

REFERENCES

Ambrose-Lanci, L. M., Sterling, R. C., & Bockstaele, E. J. V. (2010). Cocaine withdrawal-induced anxiety in females: Impact of circulating estrogen and potential use of delta-opioid receptor agonists for treatment. *Journal of Neuroscience Research*, *88*, 816–824.

Bals-Kubik, R., Shippenberg, T. S., & Herz, A. (1990). Involvement of central mu and delta opioid receptors in mediating the reinforcing effects of beta-endorphin in the rat. *European Journal of Pharmacology*, *175*, 63–69.

Bardoni, R., Tawfik, V. L., Wang, D., François, A., Solorzano, C., Shuster, S. A., … Scherrer, G. (2014). Delta opioid receptors presynaptically regulate cutaneous mechanosensory neuron input to the spinal cord dorsal horn. *Neuron*, *81*, 1312–1327. https://doi.org/10.1016/j.neuron.2014.01.044

Benbouzid, M., Gaveriaux-Ruff, C., Yalcin, I., Waltisperger, E., Tessier, L.-H., Muller, A., … Barrot, M. (2008). Delta-opioid receptors are critical for tricyclic antidepressant treatment of neuropathic allodynia. *Biological Psychiatry*, *63*, 633–636.

Brackley, A. D., Gomez, R., Akopian, A. N., Henry, M. A., & Jeske, N. A. (2016). GRK2 constitutively governs peripheral delta opioid receptor activity. *Cell Reports*, *16*, 2686–2698.

Cahill, C. M., Holdridge, S. V., & Morinville, A. (2007). Trafficking of δ-opioid receptors and other G-protein-coupled receptors: Implications for pain and analgesia. *Trends in Pharmacological Sciences*, *28*(1), 23–31.

Cahill, C. M., McClellan, K. A., Morinville, A., Hoffert, C., Hubatsch, D., O'Donnell, D., & Beaudet, A. (2001). Pattern of expression of engrailed in relation to gamma-aminobutyric acid immunoreactivity in the central nervous system of the adult grasshopper. *Journal of Comparative Neurology*, *440*(1), 85–96.

Cahill, C. M., Morinville, A., Hoffert, C., O'Donnell, D., & Beaudet, A. (2003). Up-regulation and trafficking of δ opioid receptor in a model of chronic inflammation: Implications for pain control. *Pain*, *101*(1), 199–208. https://doi.org/10.1016/S0304-3959(02)00333-0

Cahill, C. M., Morinville, A., Lee, M.-C., Vincent, J.-P., Collier, B., & Beaudet, A. (2001). Prolonged morphine treatment targets δ opioid receptors to neuronal plasma membranes and enhances δ-mediated antinociception. *Journal of Neuroscience*, *21*(19), 7598–7607. https://doi.org/10.1523/JNEUROSCI.21-19-07598.2001

Carrillo, P., Camacho, M., Manzo, J., Martinez-Gomez, M., Salas, M., & Pacheco, P. (1998). Cutaneous wounds produced by capsaicin treatment of newborn rats are due to trophic disturbances. *Neurotoxicology and Teratology*, *20*, 75–81.

Chaplan, S. R., Bach, F. W., Pogrel, J. W., Chung, J. M., & Yaksh, T. L. (1994). Quantitative assessment of tactile allodynia in the rat paw. *Journal of Neuroscience Methods*, *53*, 55–63.

Choucair-Jaafar, N., Salvat, E., Freund-Mercier, M.-J., & Barrot, M. (2014). The antiallodynic action of nortriptyline and terbutaline is mediated by beta(2) adrenoceptors and delta opioid receptors in the ob/ob model of diabetic polyneuropathy. *Brain Research*, *1546*, 18–26.

Chu, K. L., Faltynek, C. R., Jarvis, M. F., & McGaraughty, S. (2004). Increased WDR spontaneous activity and receptive field size in rats following a neuropathic or inflammatory injury: Implications for mechanical sensitivity. *Neuroscience Letters*, *372*, 123–126.

Chung, P. C. S., Keyworth, H. L., Martin-Garcia, E., Charbogne, P., Darcq, E., Bailey, A., … Gaveriaux-Ruff, C. (2015). A novel anxiogenic role for the delta opioid receptor expressed in GABAergic forebrain neurons. *Biological Psychiatry*, *77*, 404–415.

Conibear, A. E., Asghar, J., Hill, R., Henderson, G., Borbely, E., Tekus, V., … von Mentzer, B. (2020). A novel G protein-biased agonist at the delta opioid receptor with analgesic efficacy in models of chronic pain. *Journal of Pharmacology and Experimental Therapeutics*, *372*, 224–236.

Connelly, K. L., & Unterwald, E. M. (2019). Regulation of CRF mRNA in the rat extended amygdala following chronic cocaine: Sex differences and effect of delta opioid receptor agonism. *International Journal of Neuropsychopharmacology*, *23*(2), 117–124.

Drake, M. T., Shenoy, S. K., & Lefkowitz, R. J. (2006). Trafficking of G protein-coupled receptors. *Circulation Research*, *99*, 570–582.

Dripps, I. J., & Jutkiewicz, E. M. (2018). Delta opioid receptors and modulation of mood and emotion. *Handbook of Experimental Pharmacology*, *247*, 179–197.

Gaveriaux-Ruff, C., Nozaki, C., Nadal, X., Hever, X. C., Weibel, R., Matifas, A., … Maldonado, R. (2011). Genetic ablation of delta opioid receptors in nociceptive sensory neurons increases chronic pain and abolishes opioid analgesia. *Pain*, *152*, 1238–1248.

Gendron, L., Cahill, C. M., Zastrow, M. V., Schiller, P. W., & Pineyro, G. (2016). Molecular pharmacology of δ-opioid receptors. *Pharmacological Reviews*, *68*(3), 631–700.

Gendron, L., Esdaile, M. J., Mennicken, F., Pan, H., O'Donnell, D., Vincent, J.-P., … Beaudet, A. (2007). Morphine priming in rats with chronic inflammation reveals a dichotomy between antihyperalgesic and antinociceptive properties of deltorphin. *Neuroscience*, *144*(1), 263–274. https://doi.org/10.1016/j.neuroscience.2006.08.077

Gilron, I., Watson, C. P. N., Cahill, C. M., & Moulin, D. E. (2006). Neuropathic pain: A practical guide for the clinician. *Canadian Medical Association Journal*, *175*(3), 265–275. https://doi.org/10.1503/cmaj.060146

Hao, J. X., Yu, W., & Xu, X. J. (1998). Evidence that spinal endogenous opioidergic systems control the expression of chronic pain-related behaviors in spinally injured rats. *Experimental Brain Research*, *118*, 259–268.

Henry, M. S., Gendron, L., Tremblay, M.-E., & Drolet, G. (2017). Enkephalins: Endogenous analgesics with an emerging role in stress resilience. *Neural Plasticity*, *2017*, 1546125.

Hjerling-Leffler, J., Alqatari, M., Ernfors, P., & Koltzenburg, M. (2007). Emergence of functional sensory subtypes as defined by transient receptor potential channel expression. *Journal of Neuroscience*, *27*, 2435–2443.

Holdridge, S. V., & Cahill, C. M. (2007). Spinal administration of a δ opioid receptor agonist attenuates hyperalgesia and allodynia in a rat model of neuropathic pain. *European Journal of Pain*, *11*(6), 685–693. https://doi.org/10.1016/j.ejpain.2006.10.008

Hurley, R. W., & Hammond, D. L. (2000). The analgesic effects of supraspinal mu and delta opioid receptor agonists are potentiated during persistent inflammation. *Journal of Neuroscience*, *20*, 1249–1259.

Hutcheson, D. M., Matthes, H. W., Valjent, E., Sánchez-Blázquez, P., Rodríguez-Díaz, M., Garzón, J., … Maldonado, R. (2001). Lack of dependence and rewarding effects of deltorphin II in mu-opioid receptor-deficient mice. *European Journal of Neuroscience*, *13*, 153–161.

Kabli, N., & Cahill, C. M. (2007). Anti-allodynic effects of peripheral delta opioid receptors in neuropathic pain. *Pain*, *127*, 84–93.

Katz, N. (2002). The impact of pain management on quality of life. *Journal of Pain and Symptom Management*, *24*, S38–S47.

Lee, M.-C., Cahill, C. M., Vincent, J.-P., & Beaudet, A. (2002). Internalization and trafficking of opioid receptor ligands in rat cortical neurons. *Synapse*, *43*(2), 102–111. https://doi.org/10.1002/syn.10014

Liu, S. (. S., Pickens, S., Burma, N. E., Ibarra-Lecue, I., Yang, H., Xue, L., … Cahill, C. M. (2019). Kappa opioid receptors drive a tonic aversive component of chronic pain. *Journal of Neuroscience*, *39*(21), 4162–4178.

Lutz, P.-E., & Kieffer, B. L. (2013). Opioid receptors: Distinct roles in mood disorders. *Trends in Neurosciences*, *36*, 195–206.

Martinez-Navarro, M., Cabanero, D., Wawrzczak-Bargiela, A., Robe, A., Gaveriaux-Ruff, C., Kieffer, B. L., … Maldonado, R. (2019). Mu and delta opioid receptors play opposite nociceptive and behavioural roles on nerve-injured mice. *British Journal of Pharmacology*, *177*(5), 1187–1205.

McDougal, D. B. J., Yuan, M. J., Dargar, R. V., & Johnson, E. M. J. (1983). Neonatal capsaicin and guanethidine and axonally transported organelle-specific enzymes in sciatic nerve and in sympathetic and dorsal root ganglia. *Journal of Neuroscience*, *3*, 124–132.

Mitchell, J. M., Margolis, E. B., Coker, A. R., Allen, D. C., & Fields, H. L. (2014). Intra-VTA deltorphin, but not DPDPE, induces place preference in ethanol-drinking rats: Distinct DOR-1 and DOR-2 mechanisms control ethanol consumption and reward. *Alcoholism, Clinical and Experimental Research*, *38*, 195–203.

Mittal, N., Roberts, K., Pal, K., Bentolila, L. A., Fultz, E., Minasyan, A., … Walwyn, W. (2013). Select G-protein-coupled receptors modulate agonist-induced signaling via a ROCK, LIMK, and β-arrestin 1 pathway. *Cell Reports*, *5*(4), 1010–1021.

Morinville, A., Cahill, C. M., Aibak, H., Rymar, V. V., Pradhan, A., Hoffert, C., … Clarke, P. B. (2004). Morphine-induced changes in δ opioid receptor trafficking are linked to somatosensory processing in the rat spinal cord. *Journal of Neuroscience*, *24*, 5549–5559.

Nadal, X., Banos, J.-E., Kieffer, B. L., & Maldonado, R. (2006). Neuropathic pain is enhanced in delta-opioid receptor knockout mice. *European Journal of Neuroscience*, *23*, 830–834.

Overland, A. C., Kitto, K. F., Chabot-Dore, A.-J., Rothwell, P. E., Fairbanks, C. A., Stone, L. S., & Wilcox, G. L. (2009). Protein kinase C mediates the synergistic interaction between agonists acting at alpha2-adrenergic and delta-opioid receptors in spinal cord. *Journal of Neuroscience*, *29*, 13264–13273.

Pertovaara, A., Kontinen, V. K., & Kalso, E. A. (1997). Chronic spinal nerve ligation induces changes in response characteristics of nociceptive spinal dorsal horn neurons and in their descending regulation originating in the periaqueductal gray in the rat. *Experimental Neurology*, *147*, 428–436.

Pradhan, A. A., Befort, K., Nozaki, C., Gavériaux-Ruff, C., & Kieffer, B. L. (2011). The delta opioid receptor: An evolving target for the

treatment of brain disorders. *Trends in Pharmacological Sciences*, *32*, 581–590.

Pradhan, A. A., Smith, M. L., Zyuzin, J., & Charles, A. (2014). delta-Opioid receptor agonists inhibit migraine-related hyperalgesia, aversive state and cortical spreading depression in mice. *British Journal of Pharmacology*, *171*, 2375–2384.

Ribeiro-da-Silva, A., & De Koninck, Y. (2008). Morphological and neurochemical organization of the spinal dorsal horn. In A. I. Basbaum, A. Kaneko, G. M. Shepherd, & G. Westheimer (Eds.), *The senses: A comprehensive reference* (Vol. *5*, pp. 279–310). San Diego, CA: Academic Press.

Richards, E. M., Mathews, D. C., Luckenbaugh, D. A., Ionescu, D. F., Machado-Vieira, R., Niciu, M. J., … Maciag, C. (2016). A randomized, placebo-controlled pilot trial of the delta opioid receptor agonist AZD2327 in anxious depression. *Psychopharmacology*, *233*, 1119–1130.

Scadding, J. W. (1980). The permanent anatomical effects of neonatal capsaicin on somatosensory nerves. *Journal of Anatomy*, *131*, 471–482.

Scherrer, G., Imamachi, N., Cao, Y.-Q., Contet, C., Mennicken, F., O'Donnell, D., … Basbaum, A. I. (2009). Dissociation of the opioid receptor mechanisms that control mechanical and heat pain. *Cell*, *137*, 1148–1159.

Shields, S. D., Ahn, H.-S., Yang, Y., Han, C., Seal, R. P., Wood, J. N., … Dib-Hajj, S. D. (2012). Nav1.8 expression is not restricted to nociceptors in mouse peripheral nervous system. *Pain*, *153*, 2017–2030.

Sotgiu, M. L., Valente, M., Caramenti, G. C., & Biella, G. E. M. (2006). Heterotopic inputs facilitate poststimulus afterdischarges of spinal WDR neurons in rats with chronic nerve constriction. *Brain Research*, *1099*, 97–100.

Spahn, V., & Stein, C. (2017). Targeting delta opioid receptors for pain treatment: Drugs in phase I and II clinical development. *Expert Opinion on Investigational Drugs*, *26*, 155–160.

Stewart, P. E., & Hammond, D. L. (1994). Activation of spinal delta-1 or delta-2 opioid receptors reduces carrageenan-induced hyperalgesia in the rat. *Journal of Pharmacology and Experimental Therapeutics*, *268*, 701–708.

Taylor, A. M. W., Castonguay, A., Taylor, A. J., Murphy, N. P., Ghogha, A., Cook, C., … Cahill, C. M. (2015). Microglia disrupt mesolimbic reward circuitry in chronic pain. *Journal of Neuroscience*, *35*, 8442–8450.

Thomas, D. A., Dubner, R., & Ruda, M. A. (1994). Neonatal capsaicin treatment in rats results in scratching behavior with skin damage: Potential model of non-painful dysesthesia. *Neuroscience Letters*, *171*, 101–104.

Turner, K. M., & Burne, T. H. J. (2014). Comprehensive behavioural analysis of Long Evans and Sprague-Dawley rats reveals differential effects of housing conditions on tests relevant to neuropsychiatric disorders. *PLoS One*, *9*, e93411.

Vicente-Sanchez, A., Segura, L., & Pradhan, A. A. (2016). The delta opioid receptor tool box. *Neuroscience*, *338*, 145–159.

Wang, D., Tawfik, V. L., Corder, G., Low, S. A., Francois, A., Basbaum, A. I. & Scherrer, G. (2018). Functional divergence of delta and mu opioid receptor organization in CNS pain circuits. *Neuron*, *98*, 90–108.e5.

Willis, W. D. J. (1985). Pain pathways in the primate. *Progress in Clinical and Biological Research*, *176*, 117–133.

Willis, W. D., & Coggeshall, R. E. (1991). *Sensory mechanisms of the spinal cord* (2nd ed.). New York, NY: Plenum Press.

SUPPORTING INFORMATION

Additional supporting information may be found online in the Supporting Information section.

FIGURE S1 DOR antisera specificity. Immunocytochemical specificity of DOR antisera. HEK-293 cells were transfected transiently with mDOR-Myc cDNA and labeled immunocytochemically for both the DOR using the Chemicon antibody (a) and the FLAG epitope (b), followed by subsequent visualization by confocal microscopy. (c) Co-localization shows completed overlap between DOR antisera labeling and the FLAG epitope. (d) No antisera labeling was present in non-transfected HEK cells. (e) The presence of the receptor is visualized within the intracellular compartment following vehicle or DOR agonist (SNC80 1 μM) treatment for 30 min prior to fixation, indicating internalization induced by the formation of ligand-receptor complexes. All images are presented as single optical sections. Scale bar 10 μm (f, g) Identification of DOR by Western blotting. Membranes prepared from dorsal root ganglia (DRG) (lanes i, ii) and spinal cord tissue (lanes iii, iv) were resolved, probed, and blotted with the Chemicon DOR antiserum (f) or the antiserum pre-adsorbed with the antigenic peptide (g). Specific bands were detected at estimated molecular weights of 52 and 68 kDa. Pre-adsorption of antisera resulted in a reduction of all molecular species identified by immunoblotting. DOR, delta opioid receptor; HEK, human embryonic kidney

FIGURE S2 Effects of DOR agonists on mechanical withdrawal thresholds in sham animals. Mechanical withdrawal responses were assessed in Sprague Dawley rats with sham surgery, prior to and following intrathecal (i.t.) administration of DOR agonists DSLET (10 μg), DPDPE (10 μg), SNC80 (30 μg), and deltorphin (DLT, 10 μg) on day 14 post-surgery. Sham animals did not show pain hypersensitivity at 14 days following surgery (no nerve manipulation) and had pre-drug thresholds similar to baseline values of 15 g. No drug effect was noted for any of the DOR agonists. Data represent means ± *SD*s for N = 6 per group

FIGURE S3 Preconditioning times for data presented in Figure 2. Preconditioning was determined for 30 min the day immediately before drug assignment and conditioning to respective groups. All conditioning was balanced for unbiased conditioning to drug. Data is presented as raw scatter plot with means ± *SD*s

FIGURE S4 Ultrastructural images of superficial dorsal horn of the spinal cord of neuropathic pain and sham control Sprague Dawley rats. Electron photomicrographs showing the subcellular localization of DOR immunoreactivity within laminae I-II dendrites from sham (a) and day 14 neuropathic (b: ipsilateral, c: contralateral) rats. Silver-intensified gold particles occur at predominantly intracellular sites in all groups. Arrows indicate gold particles associated with the plasma membrane. At, axon terminal; D, dendrite. Scale bar = 2 μm

Transparent Peer Review Report

Transparent Science Questionnaire for Authors

Supplementary Material

How to cite this article: Cahill CM, Holdridge SV, Liu S, et al. Delta opioid receptor activation modulates affective pain and modality-specific pain hypersensitivity associated with chronic neuropathic pain. *J Neurosci Res*. 2020;00:1–20. https://doi.org/10.1002/jnr.24680